Elucidating excited state electronic structure and intercomponent interactions in multicomponent and supramolecular systems

Wesley R. Browne,[a] Noel M. O'Boyle,[b] John J. McGarvey[c] and Johannes G. Vos*[d]

Received 30th April 2005
First published as an Advance Article on the web 24th June 2005
DOI: 10.1039/b400513a

Rational design of supramolecular systems for application in photonic devices requires a clear understanding of both the mechanism of energy and electron transfer processes and how these processes can be manipulated. Central to achieving these goals is a detailed picture of their electronic structure and of the interaction between the constituent components. We review several approaches that have been taken towards gaining such understanding, with particular focus on the physical techniques employed. In the discussion, case studies are introduced to illustrate the key issues under consideration.

1. Introduction

Molecular devices, based on supramolecular (multicomponent) assemblies employing covalent and non-covalent bonds between components, are of increasing interest in the development of molecular electronics and photonic devices. One of the primary goals behind the construction of supramolecular systems is to control the direction and rate of electron and energy transfer processes, both energetically and spatially.[1] Although the energetic characteristics of these systems can be manipulated relatively easily, spatial control, in terms of both direction and rate, of energy and electron transfer can be achieved only when the orbital nature of both ground and excited electronic states is understood.

Multinuclear transition metal complexes, such as those based on d^6 polypyridyl complexes (*i.e.*, Re(I), Ru(II), Os(II) Rh(III), Ir(III)) have received considerable attention, both in fundamental studies and for application in molecular photonics.[2] The attraction of these metal compounds arises from the well-defined electrochemical and photophysical properties of their polypyridyl complexes and the extensive synthetic chemistry available, which enables systematic tuning of these properties for particular applications.[3] An additional advantage of employing 2nd and 3rd row transition metal complexes in studying intercomponent interactions lies in the stability of these complexes in different redox states. In consequence, the present tutorial review focuses primarily on metal-centred systems. However, it must be emphasised that the techniques discussed and approaches taken in these studies are not exclusive to metal based systems but can be applied equally well to organic systems.

[a]*Organic and Molecular Inorganic Chemistry, Rijksuniversiteit Groningen, Groningen, The Netherlands*
[b]*Pharmacology Department., Conway Institute of Biomolecular & Biomedical Research, University College Dublin, Belfield, Dublin 4, Ireland*
[c]*School of Chemistry, Queen's University Belfast, Belfast, BT5 9AG, Northern Ireland, UK*
[d]*National Centre for Sensor Research, School of Chemical Sciences, Dublin City University, Dublin 9, Ireland. E-mail: han.vos@dcu.ie; Fax: 00353-1-7005503; Tel: 00353-1-7005307*

Wesley R. Browne

Wesley R. Browne obtained his primary degree in Pure and Applied Chemistry in 1999 and PhD in isotopic labelling of aromatic ligands and photophysics of inorganic complexes under the direction of Prof. Han Vos in 2002, both at Dublin City University. He carried out postdoctoral research into the ground and excited state resonance Raman spectroscopy of transition metal complexes jointly with Prof. Vos and Prof. John J. McGarvey (QUB) 2002–03. In 2003, he was appointed as a postdoctoral research fellow in the group of Prof. Dr. Ben L. Feringa, University of Groningen, where his research interests include transition metal based oxidation catalysis and electrochromic materials.

Noel M. O'Boyle

Noel O'Boyle obtained his primary degree in Chemistry from National University of Ireland, Galway in 2001. In the same year, he began a PhD at Dublin City University under the supervision of Prof. Han Vos, where he used density functional theory to study the electronic structures and Raman spectra of ruthenium complexes. After completing his PhD in 2004, he was appointed as a postdoctoral researcher in the group of Prof. Ciaran Regan in University College Dublin. His current research interests involve the application of computational techniques to systems of biological interest.

In this review, we consider the characterisation of electronic states, and the application of such information to understanding the mechanism of interaction in multi-component systems. Section 2 provides a brief overview of the theoretical aspects behind photoinduced processes. Section 3 contains a description of experimental techniques available to probe electronic excited state structure. In Section 4 a number of case studies are presented outlining how the electronic properties of compounds can be studied and how this information can be used to investigate the nature of intramolecular photoinduced processes. Special attention will be paid to the nature of intercomponent interactions both in the ground state and in the excited state.

2. Theoretical considerations

Excited state intercomponent processes can be divided into three groups, energy, electron, and proton transfer.[4] Electron transfer can itself be classified as thermal, optical[5] or photo-induced,[6] while energy transfer is generally described in terms of through-bond (Dexter) or through-space (Förster) mechanisms.[7] As more comprehensive reviews of these areas are available in the literature already, only a brief description and discussion of these processes is included here.

Energy and electron transfer processes share several features; a strong distance dependence between donor and acceptor groups, and through space and through bond mechanisms are relevant to both. In order to understand these processes, three aspects should be considered:

i) The nature of the donor state,

ii) The nature of the acceptor state,

iii) The mechanism by which the donor and acceptor communicate.

In this section these aspects are addressed, together with a brief introduction to electronic structure in polypyridyl-based transition metal complexes.

2.1 Electronic structure in heteroleptic complexes

Molecular assemblies employed as building blocks for photonic devices will, by necessity, consist of a number of different components. To create such assemblies, in general, heteroleptic metal complexes, *i.e.*, complexes containing more than one type of ligand (typically polypyridyl ligands), are employed as building blocks.

Central to the development of polypyridyl based systems is the paradigm complex $[Ru(bipy)_3]^{2+}$ (bipy = 2,2′-bipyridyl). Since the first report of luminescence from this complex by Paris and Brandt in the 1960's,[8] compounds of this type have proven a mainstay of inorganic photophysics. A central issue regarding the photophysical properties of $[Ru(bipy)_3]^{2+}$, is the nature of the lowest emissive electronic states. In particular, the degree of delocalisation of the lowest excited states (*i.e.*, whether on a single bipy ligand or delocalised over all three ligands) prompted lively debate over several decades.[9] The electronic properties of $[Ru(bipy)_3]^{2+}$ are now relatively well understood and their lower electronic state manifolds are shown in Fig. 1.[10]

The lowest energy electronic transitions of this compound are metal-to-ligand charge transfer (MLCT) in nature (*i.e.*, Ru(II)-bipy to Ru(III)-bipy$^-$). The complex shows strong emission from its ^{3}MLCT state, while thermal population of a ^{3}MC (metal centred state) determines the photostability of the complex. However, the electronic structure of heteroleptic complexes is expected to be more intricate. For example, in a complex containing different bidentate ligands (*e.g.*, $[M(A)_2(B)]^{n+}$), or tridentate ligands (*e.g.*, $[M(C)(D)]^{n+}$) the potential energy diagram will contain a ^{1}MLCT and a ^{3}MLCT

John J. McGarvey

John McGarvey obtained his PhD Physical Chemistry – in gas phase photolysis – at Queen's University Belfast and was a postdoctoral research fellow at US Army Natick Laboratories, Massachusetts before appointment as Assistant Lecturer in Chemistry at Queen's University (1967) where he is presently Professor of Physical Chemistry. He has published more than 140 refereed papers, as well as several reviews. His current research interests are in laser photochemistry and spectroscopy, with particular reference to Raman spectroscopy, including resonance Raman and surface-enhanced Raman techniques, as well as time-resolved resonance Raman methods on timescales ranging from microseconds to picoseconds and applied to the spectroscopy and photophysics of metal complex excited states.

Johannes G. Vos

Han Vos obtained his PhD in Chemistry at the University of Leiden, Netherlands, in 1978. He carried out post-doctoral work at the University of Dublin, Trinity College, 1978–1979 and 1980–1982 and the University of Fribourg, Switzerland (1979–1980). He was appointed Assistant Lecturer at Dublin City University in 1982, Lecturer in 1984, Senior Lecturer in 1987, Associate Professor in 1994 and Professor of Inorganic Chemistry in 1999. He has published over 200 refereed papers, one monograph and several book chapters. He is a member of the Royal Irish Academy. His current research interests include: the investigation of ruthenium and osmium containing polypyridyl compounds with emphasis on energy- and electron-transfer processes in supramolecular structures; deuteration and its effect on photophysical properties; and the electrochemical and photophysical properties of surfaces modified with metal complexes.

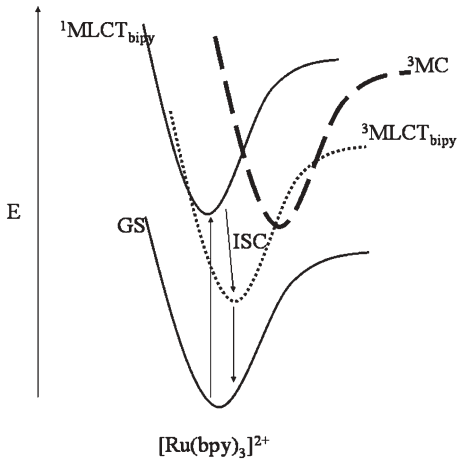

Fig. 1 Basic electronic state manifolds of $[Ru(bipy)_3]^{2+}$

energy level for each ligand. In this case it is important to know which triplet level is the lowest in energy, since, under Kasha's rule,[11] it is this level which will determine the emissive and intercomponent energy/electron transfer properties of the molecular assembly.[12] The methods available to identify the nature of the lowest excited electronic manifold will be addressed below.

2.2 Intercomponent transfer processes

Electron transfer. Electron transfer, at its simplest level, involves the movement of an electron from one point to another. In reality, however, it is better described as the movement of electron density between two components in a multi-component system (*e.g.*, D∼A, where D is the donor, A is the acceptor and ∼ the connecting bridge). In optical electron transfer (process 1 in Fig. 2) the movement of charge occurs upon absorption of a photon of suitable energy. Examples of optical electron transfer are the intervalence (IT) bands in mixed valence compounds, which are typically found in the near-IR region of the absorption spectrum.[6,13] In contrast, with photoinduced electron transfer, absorption of light creates an initial excited state (D*) in the donor component (process 2, Fig. 2) followed by thermal electron transfer (process 3, Fig. 2) to form the charge separated state ($D^+ \sim A^-$).

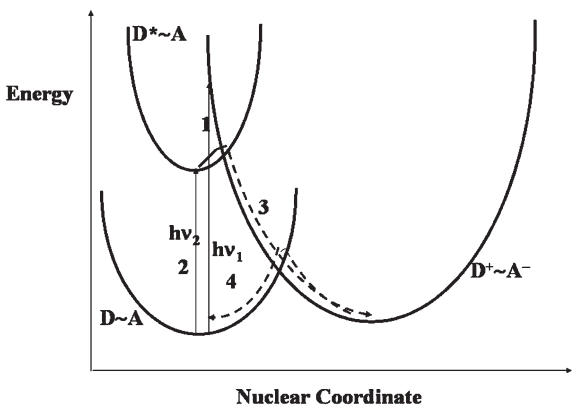

Fig. 2 Optical (1), photoinduced (2 and 3) and thermal (4) electron transfer

Energy transfer[14]. As with electron transfer, energy transfer is the movement of energy from a donor group to an acceptor group. Again, consideration of energy transfer involves understanding the energy (and orbital nature) of the donating state and of the accepting state. Equally important is that the mechanism by which energy is transferred can be described as being a combination of two limiting cases; dipole–dipole exchange (Förster) and double electron energy transfer (Dexter, Fig. 3). These limits are often described as being through space and through bond respectively. In the case of Förster energy transfer, the through-space dipole–dipole interaction is distance dependent and also dependent on the relative orientation of the interacting dipoles. Similarly, with Dexter energy transfer the rate of energy transfer (k_{EnT}) is distance dependent. However, the ability of the orbitals of the bridging unit to mediate the double electron transfer, and not the orientation of donor and acceptor dipoles, is paramount.

Ground state interaction mechanisms—HOMO *vs* LUMO superexchange processes. When the intramolecular processes in multinuclear systems are investigated it is not always appreciated that there may be differences in the interaction between the active components in the ground state and the excited state. Studies often concentrate on either the excited state (photophysics) or the ground state (electrochemistry). However, the interaction in the ground state needs to be assessed very differently from that in the excited state. In this section we will discuss, briefly, ground state interaction using models obtained from mixed valence compounds.

The observation of intervalence transitions in the near infrared region and the relationship between the properties of these transitions (*e.g.*, band width, energy, molar absorptivity, *etc.*) and the extent of interaction between the metal centres in multinuclear complexes[15] has prompted extensive studies in this area. Of particular interest is the relative delocalisation of the SOMO (singly occupied molecular orbital) over the metal centres in the mixed valence state and the mechanism of interaction in such systems, which may be through-bond (*i.e.* superexchange processes mediated *via* either the 'HOMO' or 'LUMO' of the bridging ligand) (Fig. 4) or through-space (and hence electrostatic).

The results of these studies can be extended, albeit tentatively, as a guide to the level of excited state communication between the molecular components in large systems in

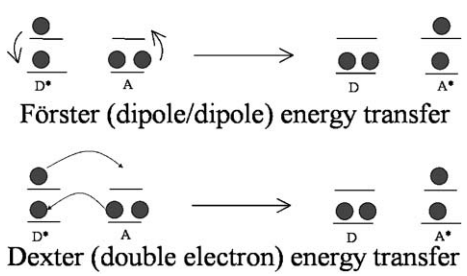

Fig. 3 Förster and Dexter energy transfer mechanisms.

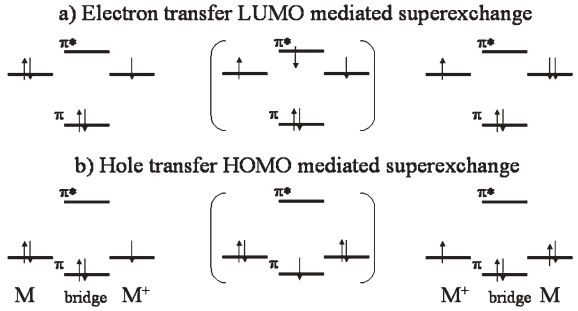

Fig. 4 a) Electron and b) hole transfer superexchange through bridging ligand π/π^* orbitals

their homovalent states (*e.g.* $Ru^{II}Ru^{II}$). This extrapolation, however, must be made with caution as it presupposes that the mechanism of interaction in the excited state is the same as or similar to that present in the mixed-valent form. For example, even in systems where the ground state communication is very weak, despite small internuclear distances, excited state communication may be strong.[16]

2.3 What is the donor–acceptor separation?

Of central importance to the understanding of electron and energy transfer processes is the effective distance over which this transfer occurs. Conventionally the donor and acceptor groups are approximated by points, typically, in the case of metal complexes, at the metal centres.[6b] In reality, however, this approximation holds only if the donor and acceptor orbitals are located entirely on the metal centres. With the exception of lanthanide-based systems, where essentially pure metal-centred (MC) excited states are involved, this is rarely the case, and indeed significant mixing of metal and ligand orbitals occurs in the majority of transition metal based systems.[18] In Fig. 5 the components of a typical transition metal based donor–acceptor system are illustrated. Given the sensitive dependence of the calculated electron and energy transfer rates on distance (*e.g.*, $1/r^6$), determining the true donor–acceptor separation is essential. The effective electron–energy transfer distance must be considered in terms of the orbital nature of the donor and acceptor states. The question then arises as to how the orbital nature of these states may be determined.

2.4 Intramolecular processes: strong *vs* weak coupling

The extent of communication between the metal centres is usually described in relative terms, as strongly coupled, weakly coupled *etc*. While undoubtedly very useful in describing and comparing related systems, the terms employed can lead to some confusion.

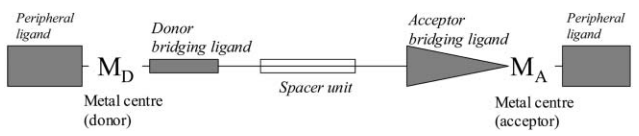

Fig. 5 Dependence of energy/electron transfer distance on location of donor and acceptor moieties in a multi-component system

In optical electron transfer, the Robin and Day[15c] classification of interaction strength is employed widely. In this classification, Type I indicates that no intercomponent interaction exists, Type III indicates that the two components interact strongly and the assembly is best viewed as a large molecule and not a multicomponent system and Type II systems exhibit a significant interaction between the components, which, however, retain the properties of the individual entities. Meyer and co-workers later introduced an additional classification, Type II/III, where the interaction can be switched between Type II and III, depending on the solvent conditions employed.[17] The strength of interaction is generally expressed using the Hush parameters, H_{ab} (in cm^{-1}) and α^2, which can be determined from a detailed analysis of the IT bands of the mixed valence compound in question.[15]

The terms 'weak' and 'strong' coupling are also used in the context of intramolecular excited state processes (*i.e.* internal conversion, IC and intersystem crossing ISC). However, in this case such descriptions refer to the nuclear displacement (*i.e.* the Huang Rhys Factor, S) of the two electronic (vibronic) states with respect to each other. For weakly coupled (or nested) states, the difference in displacement along the nuclear coordinate is small ($S < 1$), while for strongly coupled states the difference is large ($S > 1$).[18]

3. Experimental methods for the investigation of the electronic structure of compounds

The number of techniques, which have found useful application in the elucidation of electronic structure, is quite large and although most techniques are limited in what they 'see', the application of several complementary techniques to individual problems can overcome many limitations. The experimental methods can be sub-divided into steady-state and transient. However there is considerable overlap between these classifications. Thus, whilst UV-vis and emission spectroscopy are clearly steady-state techniques, they are used also encountered as transient techniques. Equally, although spectroelectrochemistry allows electrochemically generated transient (unstable) species to be probed spectroscopically, it is generally viewed as being a steady-state technique. Hence, the classification made is, in many respects, arbitrary but is retained here to help simplify the present discussion.

In the following sections, some of the more frequently encountered techniques are presented briefly with emphasis placed on the utility of these techniques in elucidating electronic structure and properties. The techniques available for probing the electronic structure of transition metal complexes include the more common steady state techniques (*e.g.*, electronic absorption, luminescence and resonance Raman spectroscopy, electrochemistry) and a range of transient techniques (*e.g.*, time resolved absorption, luminescence, infrared and resonance Raman spectroscopies). More recently other techniques such as ESR[19] spectroscopy, and, increasingly, computational methods have been applied. In addition, other strategies such as deuteration, both of solvent and ligand,[18] and acid–base[20] behaviour have proven useful in elucidating electronic structure.

3.1 Steady state techniques

Electronic spectroscopy and electrochemistry are probably the most widely used techniques in probing electronic structure. Indeed a close correlation between redox properties and electronic absorption has been observed in many cases.[21] This is not surprising as both techniques address the HOMO and LUMOs of the molecules examined. However, it must be noted that this relationship is not certain, since although oxidation involves removal of an electron from the HOMO and reduction involves addition of an electron to the LUMO, electronic absorption involves simultaneous removal of an electron from the HOMO and transfer to the LUMO. A further complication is that the lowest excited state (the THEXI or thermally equilibrated excited state) is stabilised relative to the initially populated Franck Condon state (*i.e.*, the state formed following a vertical electronic transition) and hence its orbital nature might not necessarily be identical to the LUMO level 'filled' electrochemically. In thermal (see Fig. 2), as opposed to optical, electron transfer processes [as opposed to optical], however, the LUMO level of the acceptor unit is filled in an almost equivalent way to electrochemical reduction, whilst back electron transfer to the donor HOMO is equivalent to reduction of the oxidised donor (D^+). An important consideration in assigning electrochemical processes, however, is the possibility of mixing between metal-based and ligand-based orbitals. For example, in many ruthenium–dioxolene systems the lowest oxidation processes are not exclusively ligand- or metal- centred but involve both centres. This latter aspect is treated in detail elsewhere.[22]

Resonance Raman spectroscopy[23]. Although comparison with related systems allows for a general assignment of electronic transitions in terms of the type of excited state being populated, definitive assignment cannot be made based solely on electrochemistry or UV-Vis spectroscopy. In order to make such assignments, resonance Raman spectroscopy has been employed. Raman scattering provides vibrational information complementary to IR spectroscopy but is inherently a very weak effect. However, when the excitation wavelength chosen is coincident with an electronic absorption band of a compound, enhancement (by factors up to $\sim 10^6$) of the Raman scattering from vibrational modes of the chromophore can occur. The resulting *resonance Raman* (rR) spectrum is useful in assigning electronic transitions due to the selective enhancement of vibrational bands associated with the transition. In recent years, Raman spectroscopy has undergone something of a re-birth experimentally, primarily due to the increased availability of low-cost laser sources, holographic optical filters and sensitive CCD based detectors.[23c,e]

Spectroelectrochemistry[24]. Spectroelectrochemistry involves the combination of an electrochemical technique with a spectroscopic one, so that the measurements are performed simultaneously. This allows for the *in situ* generation of synthetically inaccessible species (such as oxidised and reduced compounds), thus enabling their examination by spectroscopic techniques. In the case of optical spectroelectrochemistry the reappearance of the original spectra subsequent to electrochemical oxidation (or reduction) enables the chemical and electrochemical reversibility of a redox process to be tested. Alternatively, it can highlight chemically irreversible redox processes and provide valuable information from the resultant spectra about the constitution of the product.[25]

3.2 Transient techniques

At the most fundamental level, transient techniques involve the generation of a population inversion between the ground electronic state and higher excited states, which is then probed spectroscopically. With sufficiently long-lived species (in practice, the definition of 'long-lived' is dependent to a large extent on the equipment available!), the recovery of the ground state population can be followed with time (*i.e.*, using time-resolved techniques). In both transient and time resolved experiments, the spectra of the 'excited state species' (A*) and its evolution with time may be investigated. Almost any technique can be applied as a transient technique, *e.g.* FTIR,[26] resonance Raman,[26] UV-Vis spectroscopy and, more recently, electrochemistry.[27]

In the case of the use of resonance Raman to investigate transient species, it is important to be clear about the distinction between the two common approaches, referred to as single- and two-colour techniques, in which pulsed lasers are used to probe the Raman scattering from transients.[23c,d] In the single-colour experiment the same laser pulse populates the excited state (*i.e.* produces the transient species) and then probes the Raman (or, more usually, resonance Raman) scattering from that species (Fig. 6). Depending on the laser pulse energy (for a fixed beam diameter), the Raman (rR) spectrum will contain contributions from both the transient and parent molecular species. This single-colour approach, generally referred to as transient resonance Raman (TR^2) spectroscopy is by far the more commonly encountered transient Raman technique, often regarded as 'time-resolved', though in practice it provides little information about the dynamics of excited state processes.

True time-resolved resonance Raman (TR^3) spectroscopy involves a two-colour technique using two laser pulses, generally (but not necessarily) of different wavelength, operated in a pump-pulse delayed-probe-pulse arrangement (Fig. 7).

It is somewhat ironic that whereas infrared spectroscopy has seen much more widespread usage than Raman spectroscopy as a steady state technique, its application to time-resolved spectroscopy has been somewhat more limited. However, time-resolved IR (TRIR) has recently seen rapid developmental progress[26c] and has shown particular application to the study of carbonyl complexes, in particular rhenium(I) carbonyl complexes such as $[Re(dmb)R(CO)_3]^+$ (where dmb = 4,4′-dimethyl-2,2′-bipyridine, R = CH_3, CD_3, Et, iPr, Bz).[28a] There are also examples where both TRIR and TR^3 have been employed in a complementary manner to address photophysical problems in such systems.[28b,c]

Although many of the compounds employed in photophysical studies have singlet electronic ground states, their lowest long lived excited states are frequently not singlet,

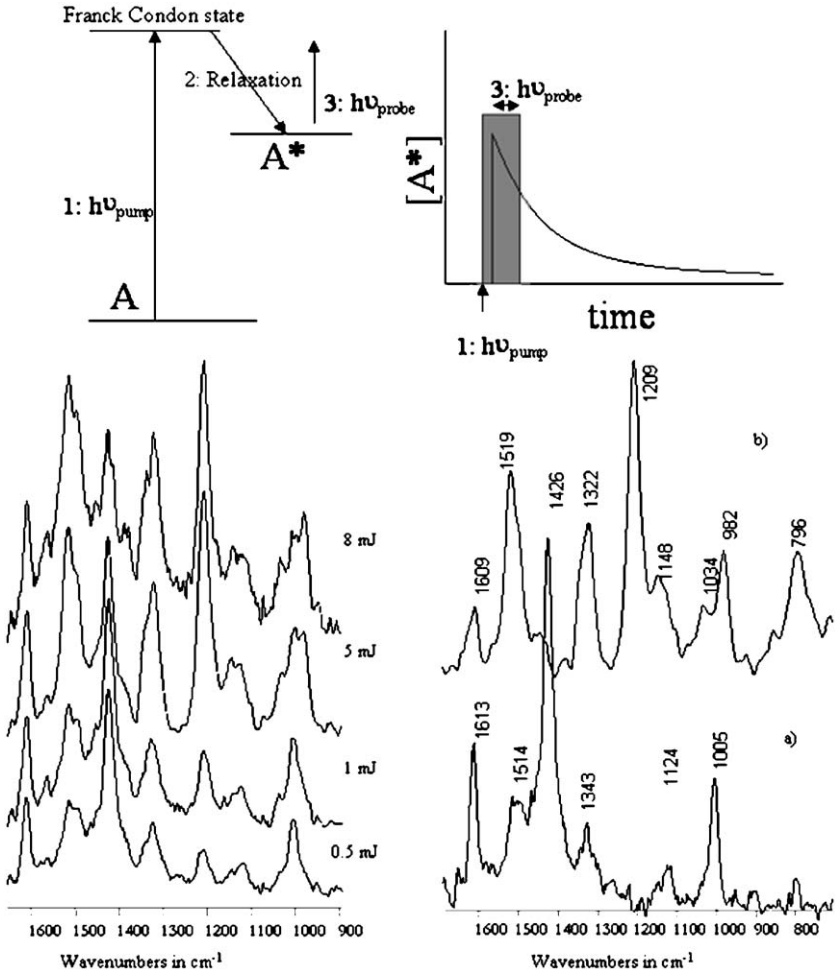

Fig. 6 Schematic diagram for a single colour 'transient' experiment. The leading edge of the excitation pulse creates (*i.e.*'pumps') A into a excited state A*, while the remainder of the pulse is used to probe the mixture of A and A* established. The [A*] present is dependent on the intensity of the excitation pulse. At low power relatively less of the sample is excited and hence mostly ground state features are observed in the spectrum generated. The proportion of excited state (A*) observed increases with increasing excitation pulse energy. By recording spectra at increasing pulse energy (a) pure ground and (b) pure excited state spectra may be obtained by spectral subtraction. Reprinted with permission from ref. 45. Copyright [2005] American Chemical Society.

particularly in the case of metal complexes, and hence may be ESR or EPR active. ESR has proven especially useful in examining long lived excited and charge-separated states.[19]

3.3 Computational techniques

Over the last decade computational (theoretical) techniques have grown from being a specialism, somewhat 'alien' to experimental chemistry, to becoming an increasingly commonplace tool in all areas of research, not least in studying electronic and redox processes. The pioneering work of J. A. Pople in the introduction and, perhaps more importantly, the objective assessment of computational models, was central to the birth and growth of this branch of chemistry, assisted by the advent of low cost high power computing resources and better graphical user interfaces.

Computational chemistry techniques are often divided into three distinct levels of theory: molecular mechanics, semi-empirical, and *ab inito*/DFT.[29] Studies of the electronic structure in large molecules such as metal polypyridyl complexes frequently use either the semi-empirical method ZINDO (Zerner's Intermediate Neglect of Differential Overlap) or density functional theory (DFT). ZINDO may be regarded as an approximation to *ab initio* theory and is parameterised to reproduce experimental results, whereas DFT is intended to be exact, although in practice approximate functionals are used.

DFT (based on the use of *functionals* linking the ground electronic state energy to the electron density) and *ab-initio* methods employ mathematical approximations to solve the time independent Schrödinger equation.[30,31]

Formally, DFT may only be used to calculate the electronic structure of the lowest energy state of each irreducible representation of the molecular point group – this is a consequence of the Hohenberg–Kohn theorem upon which modern DFT is built.[31] For a Ru(II) complex with C_1 symmetry, this means that, formally, only the singlet ground state (S_0) may be studied. However, recent studies[32] on Ru(II) polypyridyl complexes show that calculation of the lowest energy triplet state (T_1) gives energies in good agreement with

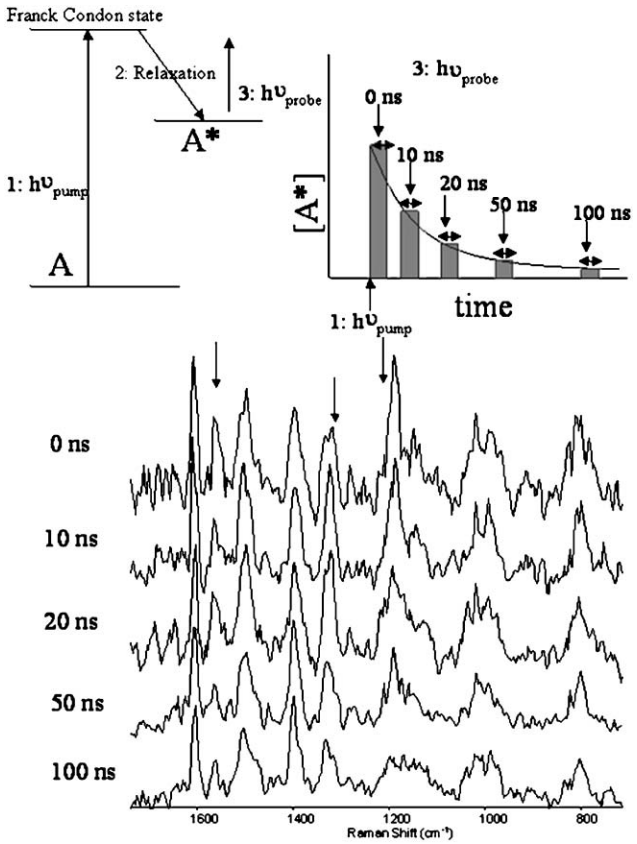

Fig. 7 Schematic diagram for a two colour 'time resolved' experiment (*i.e.* TR^3). The first pulse creates 'pumps' A into a excited state A*, while the a simultaneous pulse and further delayed pulses are used to probe the mixture of A and A* established. The [A*] present decreases with time and hence the proportion of excited state (A*) observed decreases with increasing excitation pulse delay. With time resolved spectroscopy excited state dynamics may be observed. Reprinted with permission from ref. 45. Copyright [2005] American Chemical Society.

those from time-dependent DFT (TDDFT, *vide infra*). These calculations employed the ΔSCF (self consistent field) approach,[33] where the vertical energy gap (lowest energy absorption) between S_0 and T_1 is the difference between the S_0 and T_1 energies, both evaluated at the optimised geometry of S_0 and the emission energy is the difference between the S_0 and T_1 energies, both evaluated at the optimised geometry of T_1.

3.4 Isotopic labelling

Isotopic labelling (and especially deuteration) can have a significant effect on vibrationally induced excited state non-radiative decay processes, in particular on the rates of internal conversion (IC) and intersystem crossing (ISC).[18] Many studies have been reported for organic systems but application of the strategy in inorganic chemistry has been more limited. It has been demonstrated, however, that deuteration of specific ligands in heteroleptic compounds can assist in determining the nature of the emitting state. In general it is to be expected that a deuteration effect will be observed, provided that the coupling between electronic states can be described by the weak coupling limit (*vide supra*), and provided that X–H vibrational modes make a significant contribution to the overall non-radiative rate constant ($\sum k_{nr}$). The result of this is that the location of the excited state on a particular moiety of a compound (*i.e.*, the electron density in the region of the accepting X–H oscillator) determines the extent of the effect of isotopic substitution. To a first approximation, deuteration of ligand A in the hypothetical complex $[M(A)_2(B)]$ will lead to an increase in the emission lifetime only if the emitting state is based on that ligand. Otherwise the emission lifetime will be unchanged. This behaviour is observed for many compounds and some examples will be given below. It needs to be considered, however, that coupling of excited states (*i.e.* fast internal conversion between low lying excited states[34]) may take place, in which case the results obtained may be less clear. An additional role for deuteration of ligands is encountered in rR spectroscopy. When used in conjunction with excited state rR, deuteration becomes an important tool in determining the nature of the emitting state. Since the vibrational features observed in excited state rR are related to the ligand where the excited state is located, a frequency shift in certain vibrational features upon deuteration can provide direct evidence that the excited state under investigation is localised on the deuterated ligand, as for instance in the case of a ligand radical anion in an MLCT state (*vide infra*).

3.5 Acid–base chemistry in the excited state

Upon excitation of a molecule to an electronic state above the ground state, a new molecular entity is produced with properties significantly different from those in the ground state. For example, the molecule may become simultaneously a stronger oxidising and a stronger reducing agent, its absorption spectrum will generally be changed and the acid–base properties (pK_a) may be different. The differences observed can be related directly to the differences in the electron density distribution in the molecule. These differences are particularly significant when the excited state has charge transfer character (*e.g.* MLCT, LMCT, IVCT).

The difference between ground and excited state acid–base behaviour can provide information regarding the nature of the excited state. If the compound is emissive, the excited state pK_a may be obtained from the pH dependence of the emission spectrum. Excited state pK_a values (pK_a*) have, therefore, been used to obtain information about the location of the excited state in mixed ligand complexes. It is generally observed that when the lowest energy excited state is located on the ligand with the acid–base properties, the compound becomes less acidic in the excited state than in the ground state and *vice versa* (Fig. 8a and 8b respectively). This approach has been used to determine the excited state character of a wide range of polypyridyl complexes containing ligands such as carboxy bipyridyls, triazoles, imidazoles and CN^-, which have well-defined acid–base properties.[35]

The extraction of the pK_a from emission intensity *versus* pH plots must, however, be done with consideration of the lifetime of the excited states. The best estimate is obtained from the following equation:

$$pK_a^* = pH_i + \log \tau_{acid}/\tau_{base}$$

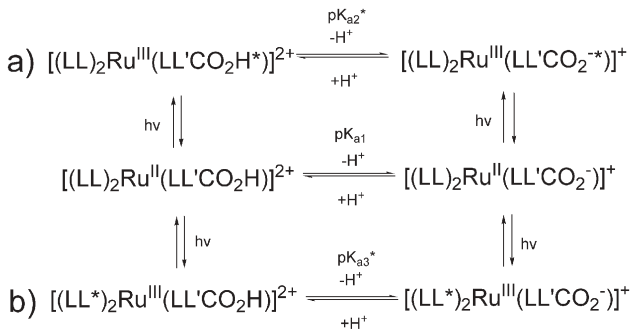

Fig. 8 Acid–base properties in the ground and lowest electronically excited state, a) where the excited state is located on a ligand bearing the 'acid/base' group, and b) where the excited state is located on a ligand not bearing the 'acid/base' group.

where pH_i is the inflection point of the emission *versus* pH plot. Excited state pK_a (pK_a^*) values can be obtained also using the difference in absorption features *via* the Förster cycle.[20] However, with this approach significant errors may be encountered. It is also important to point out that in order to obtain valid pK_a* values, an acid–base equilibrium must be established in the excited state. This may not be the case if one of the species has a very short lifetime. In that case the acid–base behaviour observed may be related to the ground state.

A further consideration is that the use of acid–base properties to help assign excited state location relies on the location of the excited state being the same in both the protonated and deprotonated excited state. This may not necessarily be the case (Fig. 9) and in this situation the interpretation of pK_a* data becomes quite challenging.

3.6 Time scale and environment

In time resolved studies, the time scale over which the experiment is conducted is important when comparing results from different techniques. Equally important is that experimental conditions (*e.g.*, solvent, concentration) be kept constant, between techniques. For example, comparing UV-Vis absorption and luminescence properties at μM concentration of a compound, which may aggregate at high concentration, with electrochemical properties measured at mM concentration is at best, unwise.

3.7 Absence of evidence is not evidence of absence

One aspect that deserves explicit mention at this point is that of the importance of a multi-technique approach to photophysical studies. For example, although both transient resonance Raman (TR^2) and luminescence spectroscopies ought to provide information regarding the same excited state, in fact, this assumes that only one excited state is populated. If

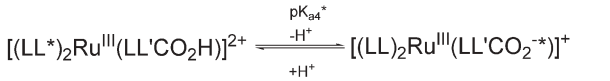

Fig. 9 Acid–base properties in the lowest electronically excited state where the location of the excited state switches between ligands depending on the protonation state.

two states (*e.g.*, one emissive and one non-emissive 'dark state') are populated to a significant level then it might be the case that the emissive state is not in resonance with the excitation laser line used in a TR^2 study. Hence, each technique will 'see' a different excited state. In most systems, where only one excited state reaches a significant population this problem does not arise. However, in multi-component systems it may become a significant issue. Ultimately, the more experimental and computational information that can be acquired about a system the more confidence that can be placed in the reliability of the resulting interpretations.

4. Case studies

In the following sections representative examples of investigations of the photophysical properties of transition metal complexes are discussed. In these examples various approaches are taken to studying electronic and photophysical properties of often complex systems. It is impossible to provide a comprehensive review of the literature in this area within the confines of the present article. Accordingly, we have selected examples from our own recent work and that of other research groups, to illustrate how experimental and computational techniques may be used to elucidate photophysical properties and intercomponent processes. Issues to be addressed include the determination of the location of the excited state in mixed ligand systems, the ability to tune the excited state properties of compounds by small variation in ligand design and the investigation of intramolecular processes between components in multinuclear systems, both in the excited state and in the ground state.

4.1 Determining the nature of the emitting state in mononuclear complexes

$[Ru(bipy)_2(pypz)]^{2+}$. Perhaps one of the simplest but informative systems to have been examined is $[Ru(bipy)_2(pypz)]^{2+}$ (see Fig. 10), where one of the pyridyl rings of $[Ru(bipy)_3]^{2+}$ is replaced by a pyrazyl ring. The question arises as to whether the lowest emissive excited state is localised on the pyrazyl ring or delocalised over the pyridyl rings. The introduction of a strong π-acceptor ligand (*i.e.*, replacement of a pyridyl moiety for a pyrazyl moiety) would be expected to have the effect of localising the lowest emissive excited state of the complex onto the pyrazyl ring, *i.e.* giving a pyrazine based ^{3}MLCT state (Fig. 10). Kincaid and co-workers have examined the spectroscopic properties (principally by resonance Raman and transient resonance Raman) of this complex in order to confirm that this is indeed the case.[36] Central to the assignment of vibrational features was the use of isotopic labelling. The resonance Raman spectra of the lowest energy absorption bands showed features typical of both pyridyl and pyrazyl rings. However, in the excited state resonance Raman spectra the characteristic bipy anion radical vibrational features (1212 cm^{-1} and 1285 cm^{-1}) were absent in the spectra of $[Ru(bipy)_2(pypz)]^{2+}$ with the spectral features of the pyridyl/pyrazyl radical anion (1212 cm^{-1} and 1277 cm^{-1}) observed instead (Fig. 11 B). The use of $[Ru([D_8]\text{-bipy})_2(pypz)]^{2+}$ and $[Ru(bipy)_2([D_2]\text{-pypz})]^{2+}$ were key to the assignment of the

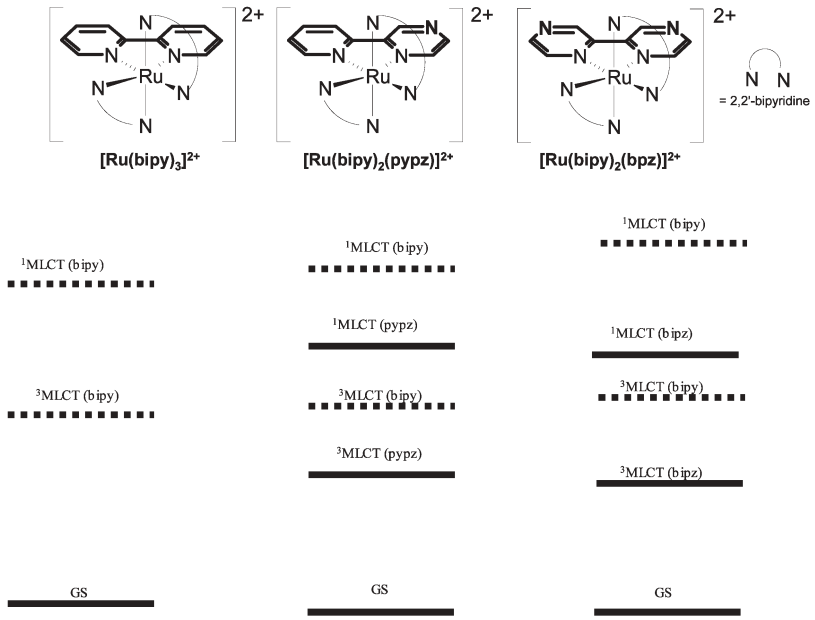

Fig. 10 Molecular structures and schematic Jablonski-type energy level diagrams of some mixed ligand ruthenium polypyridyl complexes.

lowest excited state as being localised on the pypz ligand and polarised towards the pyrazine fragment. Deuteration of the bipy ligands had no effect on the features observed in the excited state resonance Raman spectra, whereas deuteration of the pyridyl fragment of pypz ([D_2]-pypz) resulted in a modest shift in the 1212 cm^{-1} band (Fig. 11 D). Therefore, although to a first approximation the lowest ^{3}MLCT state of $[Ru(bipy)_2(pypz)]^{2+}$ may be considered to be based on the strong π-acceptor pyrazine ring, in reality the lowest ^{3}MLCT state is delocalised over the entire ligand (pypz), albeit with considerable polarisation towards the pyrazine fragment.

$[Ru(bipy)_2pytr]^+$/$[Ru(bipy)_2pztr]^+$. An extensive study of ruthenium complexes based on 1,2,4-triazole based ligands has been reported[37] (Fig. 12). The complexes $[Ru(bipy)_2(pytr)]^+$ (**1**) and $[Ru(bipy)_2(pztr)]^+$ (**2**) are almost identical in structure, differing only in the replacement of a C–H by N. The presence of the pH sensitive triazole group allows external manipulation of excited state electronic structure and considerable control over electronic and photochemical properties. In this section some of the electronic properties of these pyridine and pyrazine based complexes will be compared, with particular emphasis on the application of deuteration, acid–base properties, electrochemistry and resonance Raman spectroscopy. The influence of the protonation state of the triazole ring (Fig. 12) on the electronic properties of the compounds will also be considered.

Both **1** and **2** show very well defined redox chemistry. For both, a single metal based oxidation, Ru(II)/Ru(III), is observed at ~0.9 V *vs* SCE, with **2** being more difficult to oxidise than **1**, as expected from the increased π-acceptor properties of the pyrazine ring. For **H1** and **H2** a shift to higher potentials for the Ru(II)/Ru(III) redox process was observed, again as expected on the basis of the decreased σ-donor properties of the protonated triazole ring. The complexes are emissive both in the protonated and deprotonated state. However, the excited state acid–base chemistry of the two complexes is markedly different. For **1**, protonation to **H1** results in a blue shift in the emission and a dramatic decrease in emission lifetime.[38] In contrast for **2**, protonation to **H2** shows a modest red shift in the emission spectrum and an increase in emission lifetime. Detailed studies indicate that the excited state acidity of **1** is increased considerably while the excited state pK_a (as obtained from the investigation of the emission as a function of pH) for **2** is similar to the ground state value. These significant differences in spectroscopic behaviour were unexpected and a multi-technique approach was required to rationalise the effects observed.

Both **1** and **2** show two well-defined reduction processes at potentials almost identical to that observed for $[Ru(bipy)_3]^{2+}$. The assignment of the first reduction as being bipy based suggests that the lowest excited state will be localised on the bipy ligand. This is confirmed by the increase in emission lifetime observed upon deuteration of the bipy ligands (no increase is observed for the complexes with deuterated $pytr^-$ and $pztr^-$ ligands), and by the observation of very strong bipy radical anion features in the excited state resonance Raman spectra of the complexes (Fig. 13). In addition, for **H1** only bipy anion radical features were observed in the transient resonance Raman spectra.

However, for **H2**, excited state resonance Raman spectroscopy did not produce any evidence of bipy anion radical vibrations, and instead pyrazine anion radical features were observed (Fig. 14). This indicates that whereas for **1/H1** the lowest excited state is firmly bipy based regardless of protonation state, for **2/H2** a switching is observed upon protonation from a bipy to a pyrazine based excited state.

Spectroscopic investigation of these complexes and, in particular, temperature dependent measurements, highlights the complexity of excited electronic state structure. For example, the decrease in emission lifetime upon protonation

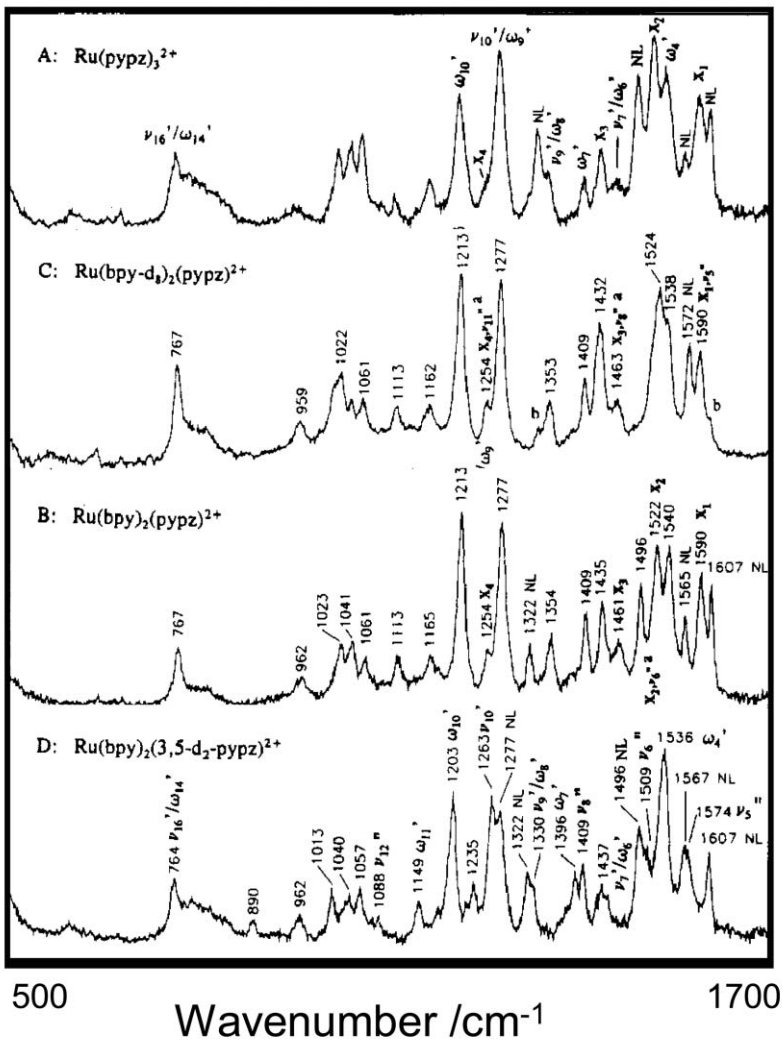

Fig. 11 TR[3] spectra of $[Ru(pypz)_3]^{2+}$, $[Ru(bipy)_2(pypz)]^{2+}$ $[Ru([D_8]\text{-}bipy)_2(pypz)]^{2+}$ and $[Ru(bipy)_2(3,5\text{-}[D_2]\text{-}pypz)]^{2+}$ acquired with 354.7-nm excitation. Reprinted with permission from ref. 36*b*. Copyright [1993] American Chemical Society.

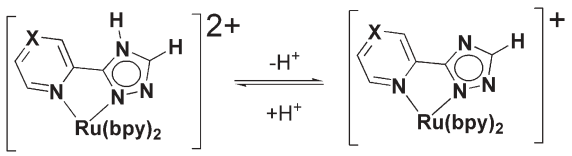

H1X = CH
H2 X = N

1X = CH
2 X = N

Fig. 12 Structures of $[Ru(bipy)_2(pytr)]^+$ and $[Ru(bipy)_2(pztr)]^+$

of **1** to **H1** is accompanied by a blue shift in emission energy. This decrease is unexpected on the basis of the well-known energy (Table 1) gap law, which would predict a lifetime increase[39] and was rationalised by assuming the involvement of a low lying ^{3}MC state, which could engage in thermally activated decay of the excited state. This explanation was verified by examination of the photochemical properties of the complexes and by temperature dependent emission spectroscopy. The data obtained indicate that for both **1** and **2** the ^{3}MC state is not populated, while for the protonated compounds this metal-centred state can be accessed thermally. This behaviour is consistent with the fact that whereas the deprotonated complexes are photostable, protonation leads to the photoinduced ligand substitution expected for compounds with accessible ^{3}MC states.

A surprising observation made for **2** is that a dual emission, with two peaks at 590 nm and 710 nm of approximately equal intensity is observed between 120 and 200 K, with the higher energy emission at 590 nm showing stronger temperature dependence than the 710 nm feature. Resonance Raman data identified the lower energy state as being bipy based. The 590 nm state was assigned as being pyrazine based (see Fig. 15).

4.2 Calculation of excited state properties by DFT

In the last few years the improved computational power of desktop computers and advances in theoretical methods have lead to an increased use of techniques such as DFT for the investigation of polypyridyl complexes. A few examples of how

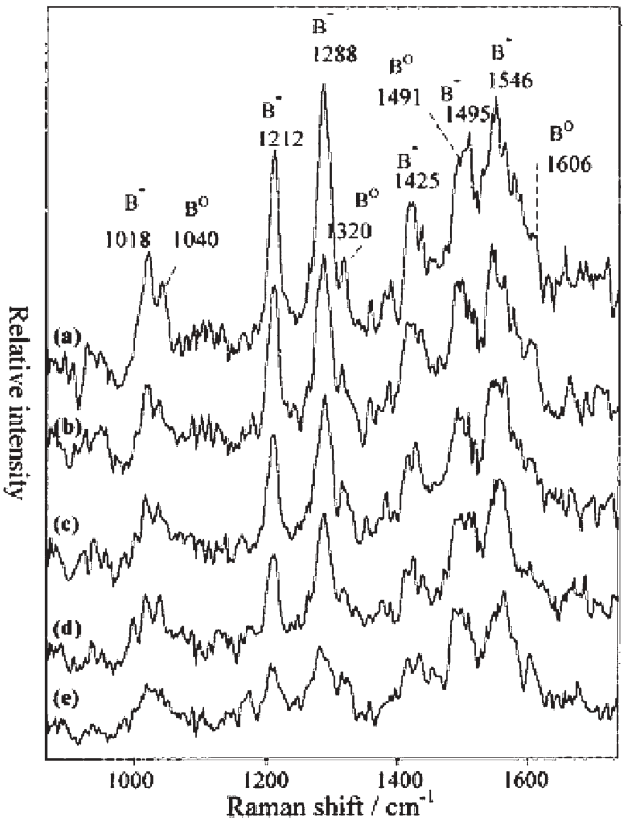

Fig. 13 Time-resolved resonance spectra of **2** in MeCN (*ca.* 10^{-3} mol dm^{-3}). Pump pulse at 355 nm (10 mJ); probe pulse 396 nm (1 mJ). Pump–probe delays in ns: (a) 10, (b) 20, (c) 40, (d) 80. (e) 396 nm probe pulse only. B^0, B^-, Z^0, Z^- denote bands attributed to neutral and anionic ligands bipy (B) and pztr (Z), respectively. Reprinted with permission from ref. 37. Copyright [1999] American Chemical Society.

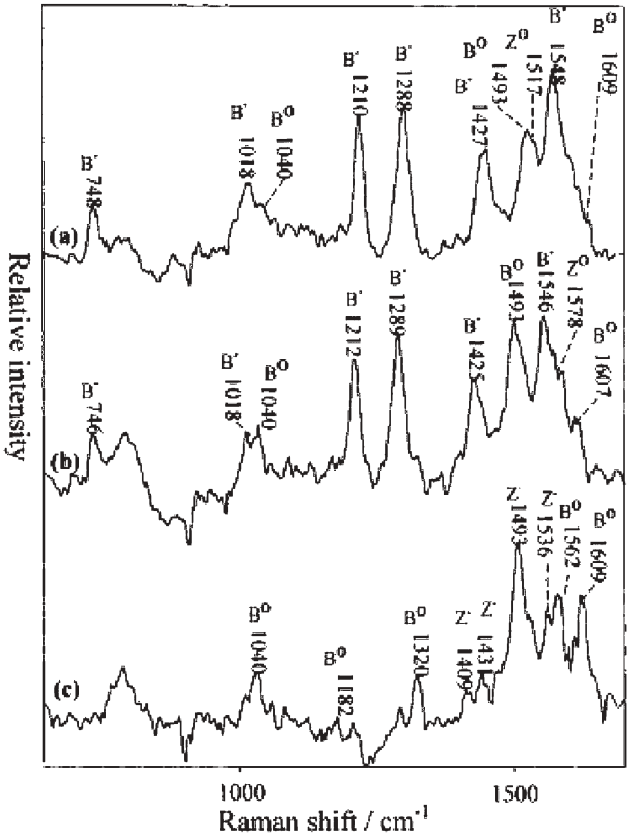

Fig. 14 Excited-state resonance Raman spectra recorded at λ_{exc} 355 nm (pulse energy 3 mJ) in MeCN, using the single-color pump and probe technique: (a) **2**; (b) **2** ([D_4]-pztr); (c) **H2**. Bands labeled as in Fig. 13. Features due to neutral bipy and anionic pztr ligands *ca.* 1493 cm^{-1} are nearly coincident. Reprinted with permission from ref. 37. Copyright [1999] American Chemical Society.

theoretical studies can be used to model excited states are discussed in this section. Daul *et al.*[40] were the first to use DFT to calculate the energies of the electronic transitions of a ruthenium polypyridyl complex, with the investigation of the MLCT manifold of $[Ru(bipy)_3]^{2+}$. Since then, time-dependent DFT (TDDFT) has been used[32,41,42] widely to investigate the excited states of Ru(II) polypyridyl complexes. TDDFT has been used to calculate the energies of the electronic transitions (both singlet and triplet) of the ground state of the complex. For example, Amini *et al.*[42] found good agreement between calculation and experiment for the energy of the ^{3}MLCT state of $[Ru(terpy)_2]^{2+}$ (16,365 cm^{-1} *vs.* 16,920 cm^{-1}). The energies of electronic transitions may also be calculated using configuration interaction (CI) and ZINDO/S, where the 'S' indicates that the method is parameterised to reproduce spectroscopic data. ZINDO/S–CI is much less computationally expensive than TDDFT and has proven very useful.[43] Using this method, Pourtois *et al.*[32c] calculated the energy of the ^{3}MLCT of $[Ru(bipy)_3]^{2+}$ to be 2.42 eV (19,520 cm^{-1} or 512 nm) at the ground state geometry.

Although the electronic structures of the excited states are not available using TDDFT or ZINDO/S–CI approaches, the electron distribution and hence the extent of localisation of the excited state may be visualised readily using electron density

Table 1 Selected emission lifetimes for **1**, **2** and **H2** and their deuteriated analogues at 298 K

Compound	τ/ns	Compound	τ/ns
$[Ru(bipy)_2(pytr)]^+$	145	$[Ru([D_8]\text{-}bipy)_2(pytr)]^+$	250
$[Ru(bipy)_2(pztr)]^+$	230	$[Ru([D_8]\text{-}bipy)_2(pztr)]^+$	290
$[Ru(bipy)_2(Hpztr)]^{2+}$	230	$[Ru(bipy)_2([D_4]\text{-}Hpztr)]^{2+}$	470

[a] Reprinted with permission from ref. 37. Copyright [1999] American Chemical Society.

difference maps (EDDMs), as shown in Fig. 16 for $[Ru(bipy)_3]^{2+}$ and $[Ru(bipy)_2(bpz)]^{2+}$ (Fig. 10). The EDDM for the lowest energy transition of $[Ru(bipy)_3]^{2+}$ (Fig. 16 (a)) shows a decrease in charge density at the metal centre, and a corresponding increase on each of the bipyridyl ligands—hence, the lowest energy transition is dRu $\rightarrow$ π*bipy MLCT. In the heteroleptic complex, $[Ru(bipy)_2(bpz)]^{2+}$, bipyrazyl is a better π acceptor than bipyridyl, and the lowest energy transition is dRu $\rightarrow$ π*bpz. This result is in agreement with the interpretation shown in Fig. 10 obtained from rR experiments. In many cases, the EDDM for the lowest energy transition can be constructed by simply subtracting the square of the HOMO, Ψ^2_{HOMO} from that of the LUMO, Ψ^2_{LUMO}. However, care is required in the case of degenerate transitions,

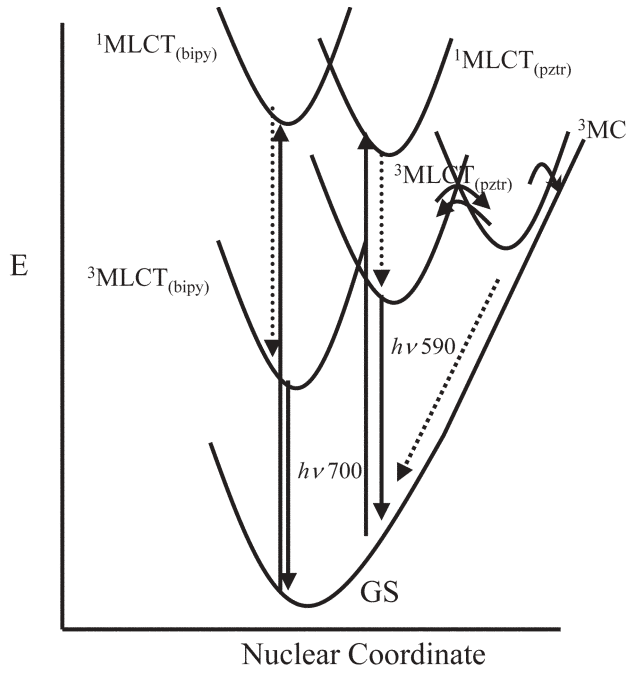

Fig. 15 Model representing the excited-state behaviour of **2**, ~ denotes nonradiative/vibrational relaxation processes. Reprinted with permission from ref. 37. Copyright [2005] American Chemical Society.

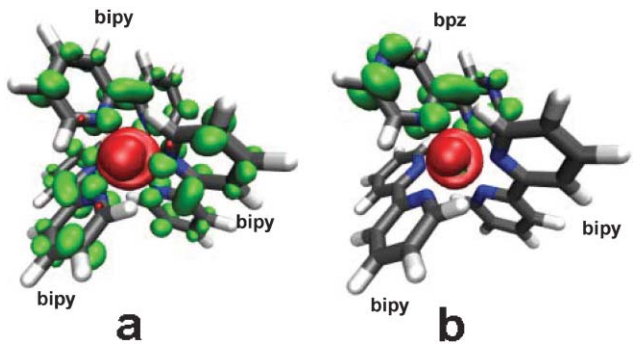

Fig. 16 Electron density difference maps (EDDMs) of the lowest energy singlet electronic transition of (a) $[Ru(bipy)_3]^{2+}$ and (b) $[Ru(bipy)_2(bpz)]^{2+}$. Red indicates a decrease in charge density, while green indicates an increase. The EDDMs were prepared from Gaussian03[58] TDDFT output (B3LYP/LanL2DZ) using GaussSum[59] and visualised using VMD[60] and PovRay[61]

and where a transition has contributions from several singly-excited configurations.[59]

A number of studies have attempted to calculate the energy of the MC (metal-centred) state of $[Ru(bipy)_2(bpz)]^{2+}$. Buchs and Daul[44] found a value of 33,000 cm^{-1} for the energy of the ^{3}MC state, computed at the geometry of the ground state. Amini *et al.*[42] used ZINDO to calculate the geometry, energy and electronic structure of the ^{3}MC state of $[Ru(terpy)_2]^{2+}$: the calculated vertical transition energy was 19,280 cm^{-1} (17,600 cm^{-1} for the relaxed ^{3}MC). Pourtois *et al.*[32c] examined the triplet excited state manifold of $[Ru(bipy)_3]^{2+}$ and $[Ru(phen)_3]^{2+}$ using ZINDOS/CI, and identified ^{3}MC transitions with energies of 3.25 eV (26,220 cm^{-1}) and 3.10 eV (25,000 cm^{-1}), respectively.

In systems of very low symmetry, computational methods become expensive in terms of computing power and the size of basis sets, which may be employed, are much lower than with homoleptic complexes. Nevertheless, computational chemistry remains of value in understanding the electronic properties of less symmetric systems.[45]

4.3 Intercomponent processes: ground state and excited state interactions in multicomponent systems

The control of interaction between units in multicomponent molecular devices is central to the development of molecular based photonics. Dinuclear compounds are ideal model systems to investigate the mechanism of both ground and excited state interaction. In a wide range of studies the nature of the bridge and the distance between the interacting components has been varied systematically to obtain information about the parameters that drive intercomponent energy and electron transfer.[22,46] A number of representative cases are discussed in this section to highlight various approaches to the design and characterisation of multicomponent systems.

The effect of the nature of the bridge on intramolecular processes. In the previous section the effect of protonation of a triazole ring on the photophysical properties of its ruthenium compounds was discussed. In this section the effect of protonation of a triazole bridge on the interaction of two ruthenium centres will be considered (Fig. 17).

As outlined above, for this particular class of compounds the electrochemical and electronic properties are dependent on the protonation state of the triazole rings and for **3** and **4** single and double protonation is possible (Table 2). Complex **3** shows two reversible protonation steps with pK_a values of 1.1 and 3.8. The pyrazine analogue, **4**, shows only minor but

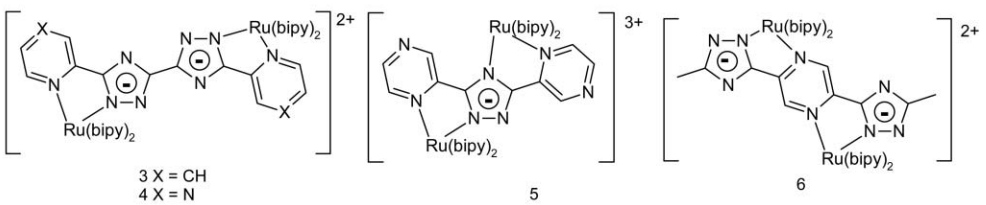

Fig. 17 Dinuclear complexes based on 1,2,4-triazole ligands.

Table 2 Electronic, photophysical and redox data in acetonitrile at 298 K for complexes **3** and **4** and their protonated analogues

	Absorption λ_{max}/nm	Emission, 298 K λ_{max}/nm, (τ/ns)	E (ox) V *vs* SCE
3	480	690 (102)	+0.80 [1], +0.98 [1]
H3	440	660 (344)	+1.06 [1], +1.17 [1]
$H_2$3	431	630 (<5 ns)	+1.10 [2]
4	455	670 (214)	+0.92 [1], +1.09 [1]
H4	436	675 (764)	+1.09 [1], +1.15 [1]
$H_2$4	430	678 (1000)	+1.13 [2]

[a] "[ ]" refers to the number of electrons under the wave. Reprinted with permission from 16*b*. Copyright [2002] American Chemical Society.

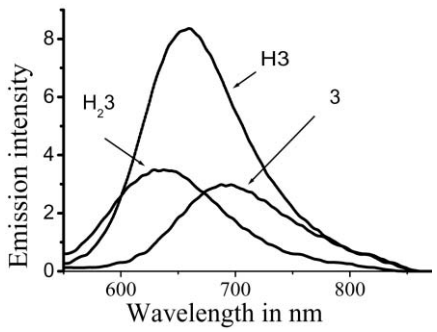

Fig. 18 Emission spectra of **3**, **H3** and **$H_2$3** in acetonitrile (protonation with CF_3SO_3H acid). Reprinted with permission from ref. 16*b*. Copyright [2002] American Chemical Society Data.

well-defined spectral changes with pH indicating the formation of **H4** and **$H_2$4** but preventing a reliable determination of pK_a values. The emission properties of **3** and **4** also show pH dependence (Table 2). Emission spectra obtained for **3** at three different protonation states are shown in Fig. 18. The emission spectrum of **3** undergoes a blue shift from 690 nm (**3**) to 660 nm (**H3**) to 630 nm (**$H_2$3**) in acetonitrile. However, for **4**, protonation results in a small red shift in the emission spectrum (*ca.* 10 nm) in agreement with observations made for other pyrazine containing triazole complexes.

For **3** and **4** two metal-based oxidation processes are observed with a gap of about 135 mV. An increase in the metal-based oxidation potentials is observed upon protonation, together with a significant decrease in the gap between the 1st and 2nd oxidation waves to less than 70 mV for **H3** and **H4** (Table 2). Both **$H_2$3** and **$H_2$4** exhibit a single two-electron metal oxidation wave. Spectroelectrochemical studies indicate the formation of intervalence bands (IT) for the deprotonated and singly protonated species. No such features are found for the fully protonated compounds. Interestingly, only minor differences are observed in the energy of the IT bands for **3** and **4** (λ_{max} *ca.* 5500 cm^{-1}) and similarly for **H3** and **H4** (λ_{max} *ca.* 8700 cm^{-1}). These data provide direct evidence for communication between the two metal centres. They also indicate that this interaction is strongly dependent on the protonation state of the bridging ligand. The effect of communication on the emission behaviour is most clearly demonstrated for **H3** (Fig. 18) and **H4**. In the absence of any interaction two emission signals are expected for a mono-protonated species. For **H3**, where the emission energy expected for the deprotonated (690 nm) and fully protonated species (630 nm) are significantly different, this would be particularly straightforward to detect. Instead, a single exponential decay of the emitting state is observed, and the λ_{max} of the emission at 660 nm is intermediate between that of **3** and **$H_2$3**. This indicates the presence of a new emitting species, in which the effect of mono-protonation is shared by both metal centres.

An important observation is that, as indicated above, the intervalence properties of **3** and **4** are very similar. This suggests that the LUMO of the bridging ligand plays at most a minor role in determining intercomponent interaction. Instead it is expected that interaction between the metal centres is taking place *via* a hole transfer mechanism as indicated in Fig. 4, involving the HOMO of the metal units and bridging ligand. This is confirmed by the decrease in interaction observed upon protonation of the bridging ligand. In a hole transfer mechanism the extent of the interaction depends on the energy gap between the dπ metal orbitals (metal-based HOMO) and the σ orbitals of the bridge. The spectroscopic and electrochemical data show that the ligand-based σ-orbitals are stabilised upon protonation, so that the energy gap between the relevant orbitals *increases*, leading to *decreased* superexchange-assisted electronic interactions.

The electrochemical and photophysical studies of these dinuclear compounds illustrate that both intercomponent interaction strength and the photophysical properties of the molecular units are "tuneable". Understanding which components dominate which processes is necessary for practical application of multicomponent systems. The close proximity of the two triazole rings creates an interaction between the two parts of the molecule. In addition, the three protonation states obtained show different levels of intercomponent interaction. It is important to note that whilst the differences in ground state properties and metal–metal interaction between the pyridine and pyrazine based complexes are minor, their luminescence properties are substantially different. Relatively small changes in the composition of the compounds, *e.g.* pyridine *vs* pyrazine lead to compounds with different excited state properties.

For complexes **3** and **4** the peripheral pyrazine/pyridine units were varied and the core triazole–triazole unit was not. The next example deals with complexes **5** and **6** and the effect of changing the bridging unit is considered. Complexes **5** and **6** are similar in composition. Both bridging ligands are based on pyrazine and 1,2,4-triazole, but these moieties are arranged in a different manner (Fig. 17). The effect of this change on the interaction in both the ground state and the excited state will be discussed. The results are compared with those reported for the Creutz–Taube ion ($[(Ru(NH_3)_5)_2(pz)]^{n+}$), for which the metal–metal distance is very similar. However, whereas the Creutz–Taube ion is non-emissive, both **5** and **6** are emissive at 670 and 748 nm respectively. For both compounds the first ligand based reduction is assigned to a pyrazine-based reduction. This suggests that the lowest excited state will be a pyrazine based ^{3}MLCT state and not a bipy based state. This is confirmed by resonance Raman spectroscopy, which shows pyrazine based vibrations.[45,47]

The overall ground state interaction between the metal centres can be obtained readily from electrochemical measurements, specifically the separation (ΔE) between the first and second metal oxidation steps. For the 1,2,4-triazolato bridged complex **5**, two metal-based oxidation processes are observed at 1.16 and 1.46 V *vs* SCE (ΔE = 300 mV). In comparison, for the pyrazine bridged complex **6**, a reduced separation is observed (ΔE = 170 mV). For the latter complex **6** the reduced separation is surprising, considering that for the Creutz–Taube ion the value observed for ΔE is 350 mV.[5] In addition, for **6**, the protonation of the triazole ring does not affect the magnitude of ΔE significantly. When compared with the general behaviour of triazole based systems discussed in the first example in this section, this is a striking observation.

These results show that while compound **6** has excited state properties which resemble those of **5**, its ground state properties are very different from those normally observed for triazole based systems. The observation that protonation does not affect the separation between the metal based redox potentials indicates that the mechanism for ground state interaction is not based on a hole transfer mechanism controlled by the bridge but that **6** behaves in this respect more like the Creutz–Taube ion with an interaction mechanism that is best explained by a LUMO based superexchange. The behaviour of the three compounds (**5**, **6**, and the CT-ion) is therefore clearly very different, despite the equivalent metal–metal separation. The importance of considering both the ground state and excited state interaction separately is further highlighted.

Energy and electron transfer in dinuclear complexes. Ruthenium(II)–osmium(II), ruthenium(II)–rhenium(I) and ruthenium(II)–rhodium(III) based dinuclear complexes are of particular interest in the study of intercomponent processes, due to the isoelectronic nature (d^6) of the four metals in the oxidation states indicated.[48] Typical examples of such mixed metal systems are shown in Fig. 19. As outlined in section 2.3 and in Fig. 5, the effective distance over which energy and electron transfer processes occur in supramolecular systems (as opposed to large molecules) is critically dependent on the location of the donor and acceptor states. Therefore, in order to understand such systems on a fundamental level, the photophysical properties of the components must first be understood. As shown in the previous section, it is possible to obtain detailed information as to the nature of the donor and acceptor excited states with the application of several complementary techniques. In supramolecular systems where understanding the properties of the individual components is essential, a second issue arises; that of the mechanism of interaction (Förster or Dexter) between the components. In addition the possibility of photoinduced electron transfer competing with energy transfer must also be considered. In this section, several examples have been chosen to illustrate various approaches taken in investigating energy and electron transfer.

Intramolecular energy transfer in phenylene bridged systems. This example deals with photoinduced energy transfer between components as a function of the orientation of the bridging ligand, *i.e.* whether the two chelating groups are *meta* (m) or *para* (p) with respect to each other (see Fig. 19). In compounds **7** and **8**[16] the distance between the metal centres is considerably larger than in the related compounds discussed in the last section. The homo-dinuclear complexes (**7a** and **7c** and **8a** and **8c**) show a single two electron redox wave at 0.84 V (**7a** and **8a**) and 0.47 V *vs* SCE (**7c** and **8c**) at potentials identical to their corresponding mononuclear complexes. In the hetero-dinuclear complexes (RuOs, **7b/8b**), the redox potentials are again identical to the respective mononuclear Ru(II) and Os(II) complexes, confirming that electronic interaction between the two metal centres in the dinuclear complexes is at most very weak and that electrostatic interaction is negligible. Spectroelectrochemical investigations of the mixed valence (*e.g.* Ru(II)Ru(III) and Ru(II)Os(III)) complexes, however, indicate that the level of electronic interaction is stronger for the *para*-phenyl substituted complexes than for the corresponding *meta*-substituted complexes. The difference in interaction is manifested in the observation of IT absorption bands in the case of *para*-substituted complexes and the absence of

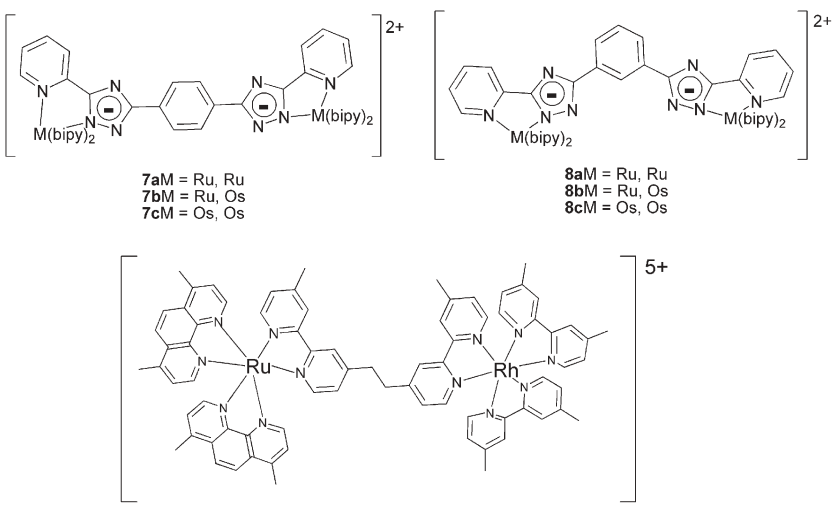

9

Fig. 19 Dinuclear complexes discussed in the text

such bands in the *meta*-substituted complexes. For the *para*-complexes, protonation of the 1,2,4-triazole groups results in a dramatic reduction in the interaction strength. The reduced interaction upon protonation and the reduced interaction observed for the *meta*-complex indicates that the mechanism of interaction is HOMO mediated through bond superexchange mechanism (*i.e.* hole transfer).

Electronic spectroscopy (absorption and emission) together with luminescence lifetime measurements have been employed to investigate energy transfer in the hetero-dinuclear complexes.[16c] The absorption spectra of equimolar solutions of the heterodinuclear complexes mRuOs (**8b**) and pRuOs (**7b**) and 1:1 mixtures of the corresponding homodinuclear species, pRuRu/pOsOs and mRuRu/mOsOs were found to be identical, in agreement with redox data. The most striking observation for these compounds is that the hetero-dinuclear complexes exhibit dual emission in all cases (*i.e.* both *meta*- and *para*-substituted and protonated/deprotonated). This is illustrated in Fig. 20. The quenching of the Ru(II) emission by the osmium centre takes place *via* an energy transfer mechanism and using standard methods[7a] the energy transfer rates can be estimated (Table 3). These values show that the energy transfer process is, predominantly, insensitive to both

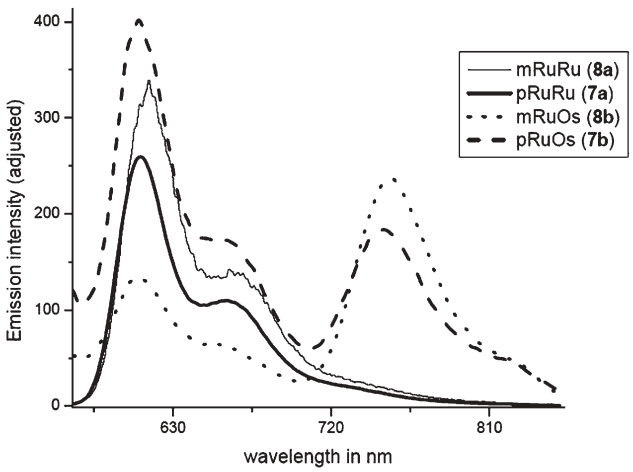

Fig. 20 Emission spectrum of dinuclear complexes at 77 K in basic ethanol/methanol 5/1 v/v. (spectral intensity is adjusted for clarity) Reprinted with permission from ref. 16*c*. Copyright [2004] American Chemical Society.

Table 3 Emission lifetimes and calculated energy transfer parameter

	τ_{em}/ns (Ru-based)	τ_{em}/ns (Os-based)	k_{EnT}/s^{-1} [b]	$k_{Förster}/s^{-1}$ [c]
7b[a]	5.7	<6	1.6×10^8	3×10^7
H7b[a]	0.6	37	$\approx 1.4 \times 10^9$	2×10^8
8b[a]	6.3	<6	1.5×10^8	3×10^7
H8b[a]	$\approx 1.0 (\approx 50\%)$; $\approx 3.0 (\approx 50\%)$	38	$(2–6) \times 10^8$	2×10^8

[a] Measured by time-correlated single-photon counting. [b] Calculated from the time-resolved data (see text). [c] Calculated using the parameters given in the Experimental section. Reprinted with permission from ref. 16*c*. Copyright [2004] American Chemical Society.

the energy of the bridging ligand HOMO/LUMO orbitals and also to orientation (*meta vs para*). This suggests that energy transfer is primarily taking place *via* a through space dipole–dipole, (Förster type) mechanism and not *via* a through bond (Dexter type) mechanism. This is in contrast to the interaction in the mixed valent state which is dominated by a through bond interaction.

Intramolecular electron transfer in Rh–Ru dinuclear systems. As an example of electron transfer processes, the hetero-dinuclear complex (**9**) (Ru(II)–Rh(III)) shown in Fig. 19 is discussed.[49] The nature of the interaction between the metal centres was established by application of a wide range of techniques including nanosecond single-photon counting (emission lifetimes), picosecond laser spectroscopy, Raman spectroscopy and transient absorption measurements.

This compound has a number of features, which make it particularly well suited for photophysical investigations. Each of the metal centres can be excited (almost) independently. Irradiation at 450 nm leads to excitation of the Ru(II) centre, while 70% of the light absorbed at 300 nm leads to excitation of the Rh(III) centre (30% goes to the Ru(II) centre). Both centres emit from long-lived triplet states and the analogous mononuclear Ru(II) and Rh(III) compounds have emission maxima at 610 nm (room temperature) and 450 nm (77 K) respectively. The Ru(II) based emission is from the lowest ^{3}MLCT state while the Rh(III) emission is ligand centred (^{3}LL) in nature.

The dinuclear compound has well-defined redox properties with a Ru(II)/(III) redox couple at 1.13 V *vs* SCE and a Rh(III)/(II) couple at −0.92 V, values which are within experimental error of the respective Ru(II) and Rh(III) mononuclear compounds. Comparison of redox and electronic data with those of the mononuclear complexes indicates that, in the ground state, the interaction between the two polypyridyl centres is, at most, weak, as expected on the basis of the saturated aliphatic nature of the bridge.

Despite such weak ground state interaction, a 90% quenching of the Ru(II) emission is observed in the Ru(II)–Rh(III) dyad (in comparison with the mononuclear Ru(II) complex). Transient resonance Raman spectroscopy identified the location of the lowest ^{3}MLCT state of the Ru(II) state as being based on the dimethyl-bipyridine of the bridging ligand and not on the peripheral dimethyl-phenanthroline ligands.

The nature of the intercomponent quenching process, *i.e.* energy *vs* electron transfer, now needs to be established. Based on the spectroscopic and redox data given above, both electron transfer to the Rh(III) moiety and energy transfer from the Ru(II) to the Rh(III) centre are thermodynamically allowed and could be responsible for the quenching process. The excitation spectrum obtained for the Ru(II) based emission contains no absorption features at 300 nm that can be related to the Rh polypyridyl moiety as would be expected for an energy transfer mechanism. Electron transfer,

$$*\text{Ru(II)–Rh(III)} \rightarrow \text{Ru(III)–Rh(II)}$$

is, therefore, the most likely explanation for the quenching process and this is confirmed by emission decay and transient absorption

spectroscopy. Picosecond laser photolysis results obtained subsequently for excitation of the Rh moiety with UV light indicated that the thermally driven back reaction:

$$\text{Ru(III)–Rh(II)} \rightarrow \text{Ru(II)–Rh(III)}$$

is faster than the forward reaction. An overall scheme of the electronic properties determined for this compound is shown in Fig. 21.

Intramolecular energy transfer in molecular dyads and triads. The importance of considering not only the relative energy of the donor and acceptor states in energy and electron transfer processes, but also the extent of localisation of these states in multicomponent systems was highlighted in recent studies by Constable and co-workers on Ru_2–Os triads[50] and by Ward and co-workers on a series of dyads based on 2-(2-pyridyl)-imidazole (PB-Ar) complexes of Re(I), Ru(II) and Pt(II), covalently connected to a series of aromatic groups (*i.e.* phenyl, pentafluorophenyl, naphthyl, anthracenyl and pyrenyl).[51]

In the case of the Re(I) and Pt(II) based complexes ([Re(PB-Ar)$(CO)_3$Cl] and [Pt(PB-Ar)$(CCR)_2$] where CCR is an acetylide ligand) the donor ^{3}MLCT state is localised on the PB ligand in very close proximity to the aryl group. In contrast, in the Ru(II) complexes (*i.e.* $[Ru(bipy)_2(PB\text{-}Ar)]^{2+}$) the donor ^{3}MLCT state is localised on the peripheral bipy ligand. For all three series of complexes strong emission {553–605 nm (Pt series), 620–640 nm (Re series) and 626–645 nm (Ru series)} arising from the ^{3}MLCT state was observed, with luminescence lifetimes of up to 500 ns and quantum yields of up to 6% in air-saturated CH_2Cl_2 at room temperature (Table 4). The ground state energy of each of the complexes (*i.e.* the metal oxidation potential) is approximately equal ($\sim$1.0 V *vs* Fc/Fc^+) and hence the ^{3}MLCT states of the Pt(II), Re(I) and Ru(II) complexes are expected to be quite close in energy. Hence, the differences in the energy transfer rates and efficiency observed can, reasonably, be assigned to differences in the separation between the donor and acceptor.

Table 4 Luminescence properties of PB complexes (CH_2Cl_2, room temperature)

Complex	λ_{em}[a]/nm	τ/ns	Φ[b]
Pt-PBPh-Py	553	404	0.054
Pt-PBPh-CF_3	560	515	0.059
Pt-PBE-CF_3	556	398	0.055
Pt-PBE-Ph	595	225	0.027
Pt-PBF-Ph	605	230	0.021
Pt-PBN-Ph	597	274	0.030
Pt-PBPh-Ph	600	278	0.027
Re-PBN	623	—	$\sim 10^{-3}$
Re-PBPh	620	—	$\sim 10^{-3}$
Re-PBF	640	—	$\sim 10^{-3}$
Re-PBA	395,418,440[c]	—	$\sim 10^{-4}$
Re-PBPyr	400	—	$\sim 10^{-4}$
Ru-PBF	645	276	0.011
Ru-PBPyr	626	356	0.011
Ru-PBA	630, 400,421,445[c]	232, 4	$\sim 10^{-3}$
Ru-PBN	630	312	0.015

[a] Emission maxima are uncorrected. [b] Quantum yields were calculated using $[Ru(bpy)_3]^{2+}$ in aerated water (Φ = 0.028) as standard. [c] Anthracene-based luminescence. Reproduced from ref. 51 with permission of the Royal Society of Chemistry. Copyright RSC 2004.

In the Re(I) and Ru(II) series there is clear evidence for inter-component energy-transfer processes in both directions between the ^{3}MLCT state of the metal centre and the singlet and triplet states of the pendant organic luminophores (naphthalene, pyrene, anthracene). For example the pyrene singlet is almost completely quenched by energy transfer to a

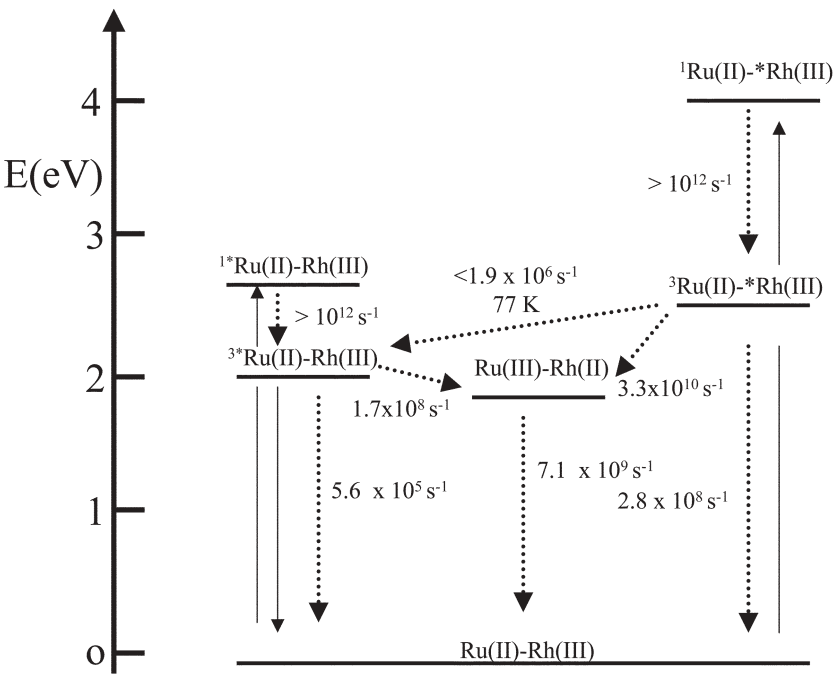

Fig. 21 Energy level diagram of the Ru(II)–Rh(III) dyad (**9**). Rate constants refer to acetonitrile solutions at 295 K, unless otherwise noted. Reprinted with permission from ref. 49. Copyright [1994] American Chemical Society.

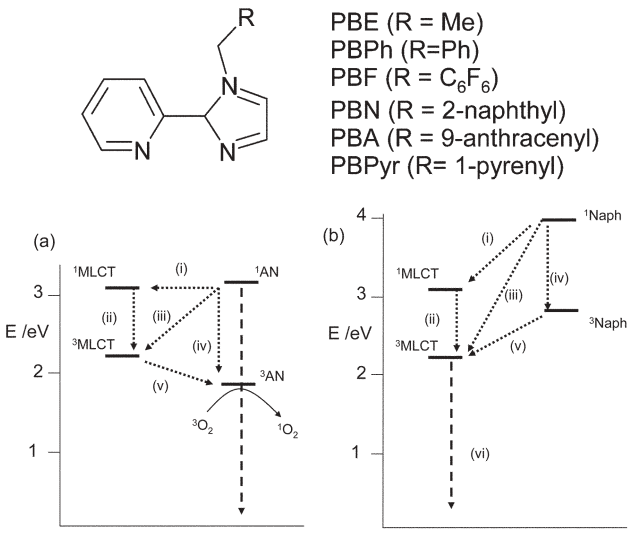

Fig. 22 Energy-level diagram for (a) Re–PBA and (b) Re–PBN. Reproduced with permission from ref. 51.

Re-based MLCT excited state, which in turn is completely quenched by energy transfer to the lower-lying pyrene triplet state (Fig. 22). For the analogous Ru(II) complexes the intercomponent energy transfer is less effective, with no observable ^{1}anthracene → Ru ^{3}MLCT energy transfer, and a reduced efficiency for Ru ^{3}MLCT → ^{3}anthracene energy transfer. This is rationalised on the basis of a greater effective distance for energy transfer in the Ru(II) series, because the MLCT excited states are localised on the bipy ligands which are remote from the pendant aromatic group; in contrast, for the Re series, the MLCT excited states involve the PB ligand to which the pendant aromatic group is attached directly, leading to more efficient energy transfer.

A similar dependence on the location of the ^{3}MLCT excited state was observed by Constable and coworkers,[50] in regard to the rate of energy transfer between Ru(II) and Os(II) terpy based complexes (Fig. 23). At room temperature the very short lifetime (<10 ns) of the donor Ru(II) ^{3}MLCT states prevent energy transfer to the lowest Os(II) ^{3}MLCT state (based on the peripheral thienyl-terpy ligand). At 77 K, energy transfer is observed due to the longer lifetime of the Ru(II) ^{3}MLCT states. However, for complex **11** the rate of energy transfer is less than for **10** due to the localisation of the ^{3}MLCT on the peripheral thienyl-terpy ligand rather than on the terpy ligand forming the bridge between the metal centres (as is the case for **10**).

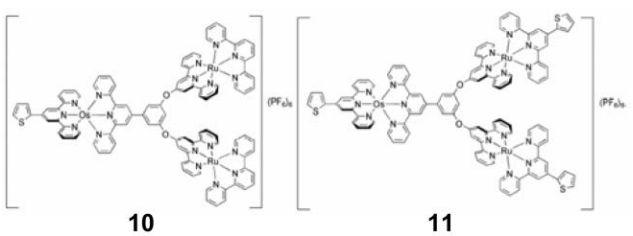

Fig. 23 Thienyl-terpy based heteromolecular triads. Reproduced with permission from ref. 50.

Energy and electron transfer in self-assembled multicomponent systems. In contrast to covalently linked multicomponent systems, the use of dynamic self-assembly introduces an added level of complexity to the investigation of excited state processes. Nevertheless this increased level of complexity, whilst requiring careful experimental control, should not limit our ability to probe energy and electron transfer processes to a similar level as in covalently tethered systems. Indeed, many examples of such detailed studies have been reported to date and in the following section a few of these are discussed.

Energy and electron transfer in hydrogen bonded systems. Energy transfer in hydrogen bonded supramolecular systems represents a challenge to spectroscopic studies due to their environmental sensitivity (*e.g.*, to trace amounts of polar and protic solvents, rapid break-up and reformation of hydrogen bonds, pH *etc.*). Nevertheless, the study of supramolecular systems based on strong hydrogen bonding interactions is an area of growing interest due to possible applications in intelligent (*i.e.*, responsive) materials and the potential for development of large systems based on non-chemically coupled subunits. Supramolecular systems of this type, however, involve equilibria between aggregate and molecular units, which must be considered in any analysis of their spectroscopic properties.

Energy transfer between Ru(II) (energy donor) and Os(II) (energy acceptor) based supramolecular complexes have been explored by Rau *et al.* (Fig. 24).[52] Although, the system studied is very sensitive to hydrogen bond disruptors (*e.g.* water), in dry aprotic solvents efficient energy transfer could be observed using a combination of luminescence and single photon counting techniques. Fig. 25 shows that while the Ru(II) emission increases linearly with concentration of the complex in the presence of $[Os(bipy)_3]^{2+}$, in the presence of $[Os(bipy)_2(mcbipy)]^{2+}$ a two step process is observed where the Ru(II) emission is initially quenched by the Os(II) complex until a ratio of ~1:1 is reached. It is worth pointing out that even in very dry CH_2Cl_2 not all of the ruthenium monomer is associated with the osmium monomer. Hence, the observation of emission from Ru(II) even in the presence of excess Os(II), does not indicate that energy transfer in the hydrogen bonded dyads is slow. From emission decay traces obtained by single

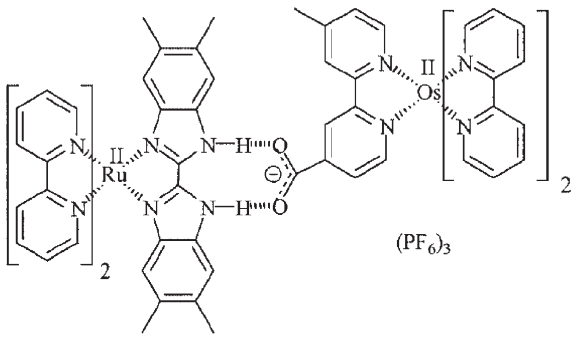

Fig. 24 Supramolecular aggregate consisting of $[Ru(bipy)_2$-(4,4′,5,5′-tetramethyl-2,2′-bibenzimidazole)$]^{2+}$, $Ru(biH_2)$, and $[Os(bipy)_2$(4-carboxy-4′-methyl-2,2′-bipy)$]^{2+}$, Os(mcbipy). Reprinted with permission from ref. 52. Copyright [2003] John Wiley & Sons, Inc.

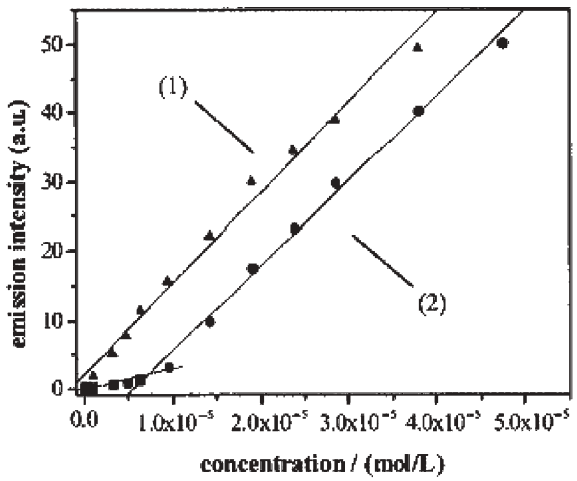

Fig. 25 Emission intensity *vs* concentration of $Ru(biH_2)$ with $[Os(bipy)_3]^{2+}$ (1) and Os(mcbipy) (2) in dichloromethane. [Os(mcbpy] = 0.95 * 10^{-6} mol L^{-1}, $[Ru(biH_2)] = x$ * [Os(mcbpy], x = 0.1, 0.33, 0.5. 0.67, 1, 1.5, 2, 2.5, 3, 4. Reprinted with permission from ref. 52. Copyright [2003] John Wiley & Sons, Inc.

photon counting both the ruthenium and osmium emission are clearly biphasic. In addition, the lifetime of the decay of the short lived process observed in the ruthenium emission is coincident with a long rise time observed for the osmium emission (see Fig. 26). This supported the conclusion that efficient but slow (ns timescale) energy transfer was occurring *via* the hydrogen-bonded bridge. This effect was lost in the presence of even trace levels of protic solvents *e.g.* methanol and no such interaction was observed with the $[Os(bipy)_3]^{2+}$, confirming the effect is not a result of a purely diffusion-controlled process.

Energy and electron transfer in self assembled Ru(II)–Ln(III) multinuclear complexes. Beer *et al.* have examined both energy and electron transfer in a series of calix[4]arene modified $[Ru(bipy)_3]^{2+}$ complexes, which are capable of binding near-Lanthanide(III) ions (*i.e.* Nd^{3+}, Eu^{3+} and Tb^{3+}).[53] The use of

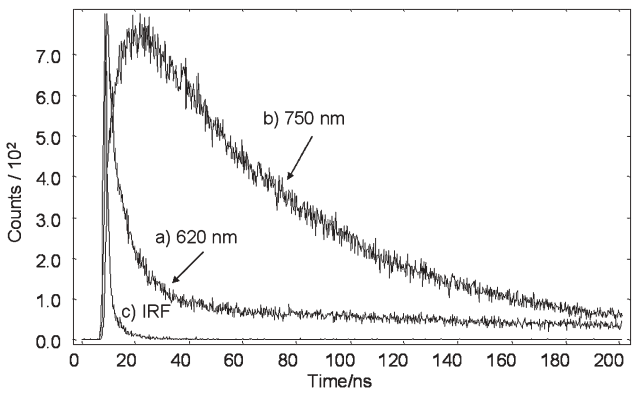

Fig. 26 Overlay of $Ru(biH_2)$ emission (a: monitored at 620 nm) and Os(mcbipy) emission (b: monitored at 750 nm) in a 1:2 ratio of the compounds, IRF (Instrument Response Function; c: monitored at 620 nm). Reprinted with permission from ref. 52. Copyright [2003] John Wiley & Sons, Inc.

lanthanides as probes in the study of energy and electron transfer offers distinct advantages over other metals, in particular the ability to tune electronic energy levels by variation in the lanthanide metal employed, with minimal differences in other physical characteristics such as binding constants, ion size and ion charge. A further advantage in using lanthanide(III) ions lies in the metal-centred (*i.e.* f–f) nature of their emissive states, which reduces uncertainty in terms of energy and electron transfer distances. By employing differing numbers of calixarene adducts (1, 2 or 6) the Ru(II):Ln(III) stoichiometry can be varied. The formation of the multi-nuclear complexes (and determination of association constants) was determined from changes in the absorption spectrum, specifically from changes in the absorption bands associated with the calix[4]arene units. The extent of quenching of the strong luminescence of the $[Ru(bipy)_3]^{2+}$ core was found to be dependent on the nature of the lanthanide ion employed ($Nd^{3+} > Eu^{3+} > Tb^{3+}$, Gd^{3+}) and in fact the luminescence was increased by the use of Tb^{3+} and Gd^{3+}.

For Nd^{3+}, the quenching of the luminescence of the $[Ru(bipy)_3]^{2+}$ core was found to occur *via* an energy transfer mechanism. Excitation spectra confirm that, although efficient energy transfer from the calix[4]arene to the Nd^{3+} is observed, the calix[4]arene units do not sensitise emission from the $[Ru(bipy)_3]^{2+}$ core. These results were rationalised on the basis of the lower energy of the Nd^{3+} ($^4F_{3/2}$) emissive excited state compared to the ^{3}MLCT state of the $[Ru(bipy)_3]^{2+}$ core and of the very efficient energy transfer from the calix[4]arene to the coordinated Nd^{3+} ion.

For Tb^{3+} and Gd^{3+} the quenching of $[Ru(bipy)_3]^{2+}$ luminescence by energy transfer is not observed, as expected, given the higher energy of the Tb^{3+} ($^5D_1$) emission. Instead, an increase in Ru(II) emission intensity and lifetime is observed. This increase cannot be attributed to thermal equilibration of the ^{3}MLCT and $^5D_1$ states given the large difference in energy. The possibility of energy transfer from the Gd(III) and Tb(III) calixarene complex to the $[Ru(bipy)_3]^{2+}$ core was excluded by examination of the excitation spectra (obtained from monitoring the emission at the λ_{max} of the Ru(II) ^{3}MLCT emission). The strong absorption band assigned to the Tb(III) calixarene complex was notably absent in the excitation spectrum obtained. In contrast, excitation spectra obtained by monitoring the λ_{max} of the Tb(III) emission confirmed that the calixarene was effective in sensitising the Tb(III) emission. On the basis of these results the extension in emission lifetime and increase in emission intensity were assigned as being due to the increased rigidity of the Ru(II) complex and the consequent reduction in the contribution of vibrational modes to the deactivation of the ^{3}MLCT excited state.[18]

In contrast to Nd^{3+}, Tb^{3+} and Gd^{3+}, for Eu^{3+}, a decrease in emission intensity of the $[Ru(bipy)_3]^{2+}$ core was observed. However, a simultaneous sensitisation in the Eu(III) emission was not observed. This effect was rationalised on the basis of electron transfer competing effectively with energy transfer processes. The low reduction potential of the Eu^{3+} ion and the strong reducing power of the Ru(II) centre in the ^{3}MLCT state make electron transfer thermodynamically very favourable. This conclusion is supported by the observation of an increase in Eu^{3+} emission intensity in frozen solutions. In rigid matrices,

stabilisation of the charge transfer state by solvent reorganisation cannot occur and hence the energy of the CT state is increased, allowing energy transfer processes to become more competitive.

The results of the study (summarised in Fig. 27) highlight the necessity of using several techniques (emission lifetime measurements, absorption, emission and excitation spectroscopy, temperature dependence studies and electrochemistry) to understand and discriminate between energy and electron transfer processes in complex and dynamic systems. In particular the consideration of the orbital parentage (*e.g.* ^{3}MLCT, ^{3}MC) of the excited states is essential.

Energy and electron transfer in dynamic self-assembled donor–acceptor arrays. Photoinduced energy and electron transfer processes in self-assembled triads based on $[Ru(bipy)_2(bpy\text{-}L)]^{2+}$ with organic donor and acceptor units bridged by trivalent (but spectroscopically silent) ions such as Sc(III), have been investigated by Kercher *et al.*[54] The Sc(III) acetyl acetonate derivative is employed to promote dyad formation due to its high association constant ($K_\beta > 10^{15}$ in water). However, the dynamic nature of this first row transition metal ion (the average lifetime of the complex is 5 ms) leads to a statistical mixture of donor–acceptor species, resulting in a challenging system for spectroscopic investigations. The $[Ru(bipy)_2(bpy\text{-}L)]^{2+}$ is capable of acting either as energy donor (with anthracene as the energy acceptor) or as electron acceptor {with *N*,*N*,*N*′,*N*′-tetramethyl-2,5-diaminobenzene (TMDAB) as electron donor}. Using emission lifetime measurements, the various photophysical processes in these kinetically labile systems could be elucidated. The choice of components is critical in reducing the complexity of the photophysical study. For example Sc(acac) complexes which incorporate three anthracene (or three TMDAB) units do not absorb at the probe wavelengths employed and, as a result, are not observable. $[Ru(bipy)_2(bpy\text{-}L)]^{2+}$ is employed as energy donor–electron acceptor due to its absorption in the visible region of the UV-Vis spectrum and its very well defined spectroscopic properties.

Intercomponent energy transfer in the $[Ru(bipy)_2(bpy\text{-}L)]^{2+}$/anthracene systems is expected to follow similar electronic energetics to those observed in covalently linked assemblies (see Fig. 28). Absorption spectroscopy confirms that no significant interaction between the donor and acceptor occurs upon mixing in a 2:1 ratio in the presence or absence of Sc(III) ions. The formation of the donor–acceptor complexes is supported by the decrease in emission from the $[Ru(bipy)_2(bpy\text{-}L)]^{2+}$site due to energy transfer to the anthracene ^{3}IL state. The possibility of energy transfer occurring through diffusional contact rather than as a result of formation of the multicomponent arrays cannot be excluded, however. The ability of anthracene (in the T_1 state) to interact with $^3O_2$ was exploited in this study to confirm the formation of the arrays. In the presence of Sc(III) ions photolysis of the solution at 460 nm (where direct excitation of anthracene cannot occur) led to a decrease in absorption features of the anthracene unit and increase in the emission intensity of

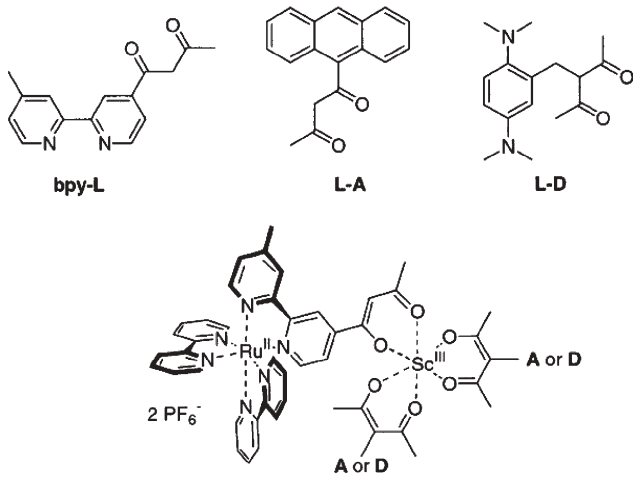

Fig. 28 Formulas of the components bpy-L, L-A, and L-D and a schematic representation of self-assembled dyads *via* the coordination to the scandium(III) ion. Reprinted with permission from ref. 54. Copyright [2002] American Chemical Society Data.

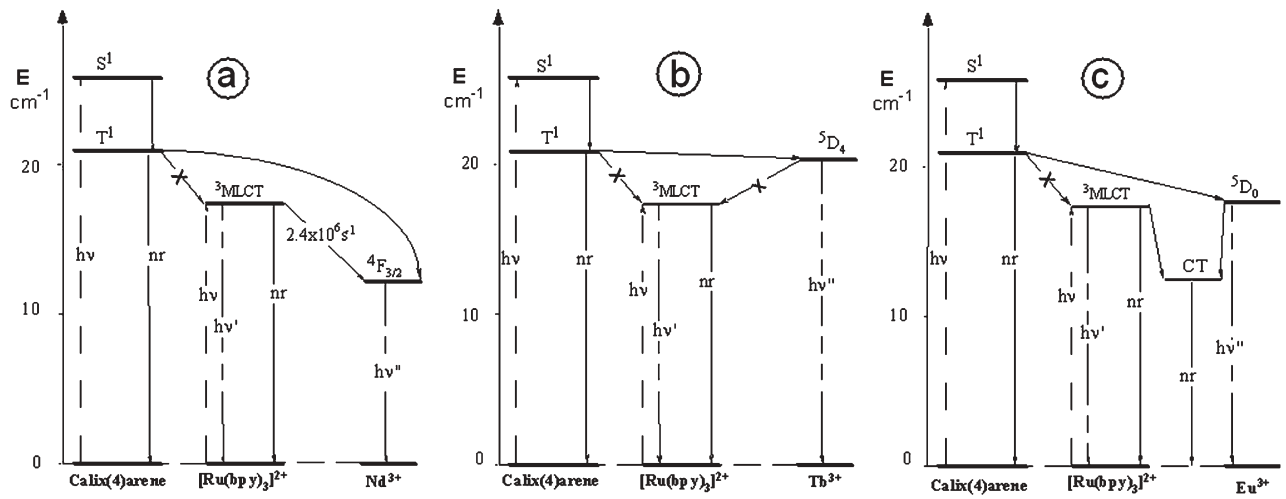

Fig. 27 Energy level diagram accounting for the photophysical behaviour of the lanthanide adducts with the ruthenium bipyridyl calix[4]arene complexes: a) Nd^{3+}, b) Tb^{3+}, c) Eu^{3+}. Reprinted with permission from ref. 53. Copyright [2004] American Chemical Society Data.

$[Ru(bipy)_2(bpy\text{-}L)]^{2+}$, due to the inability of the oxidised anthracene to act as energy acceptor (Fig. 29). Similarly in the absence of Sc(III) ions, a decrease in the absorption feature of the anthracene was observed. However in this case no increase in $[Ru(bipy)_2(bpy\text{-}L)]^{2+}$ emission was observed.

Intercomponent photoinduced electron transfer in the $[Ru(bipy)_2(bpy\text{-}L)]^{2+}$/TMDAB systems proved even more accessible than the anthracene based systems due to the very strong absorption of the TMDAB cation radical between 500 and 750 nm, which made it possible to employ time-resolved absorption spectroscopy in the study of the charge transfer state. In the absence of Sc(III) ions no quenching of the $[Ru(bipy)_2(bpy\text{-}L)]^{2+}$ emission was observed and the emission decay of the Ru(II) ^{3}MLCT state was found to be mono-exponential (150 ns in aerated acetonitrile), identical to that observed in the absence of TMDAB (Fig. 30). Under identical conditions in the presence of Sc(III) ions, clear evidence for the formation of donor–acceptor arrays was obtained from both the reduction in emission intensity and the biexponential nature of the Ru(II) ^{3}MLCT emission decay (10 ns and 150 ns, the latter being due to free $[Ru(bipy)_2(bpy\text{-}L)]^{2+}$). Transient absorption spectra recorded in both the absence and presence of Sc(III) ions, show the presence of the well known bipy radical anion (375 and 520 nm). The practical complication arising from overlap of the 520 nm band with that of the TMDAB radical cation was overcome by examination of the relative intensities of the 375 and 520 nm bands in the absence and presence of Sc(III) ions. In the presence of Sc(III) ions, the two bands are approximately equal in intensity whereas in the absence of Sc(III) the ratio is ~3:1. An analysis of the kinetics of the evolution of the transient absorption spectra gave a lifetime of ~40 ns for the charge-separated state.

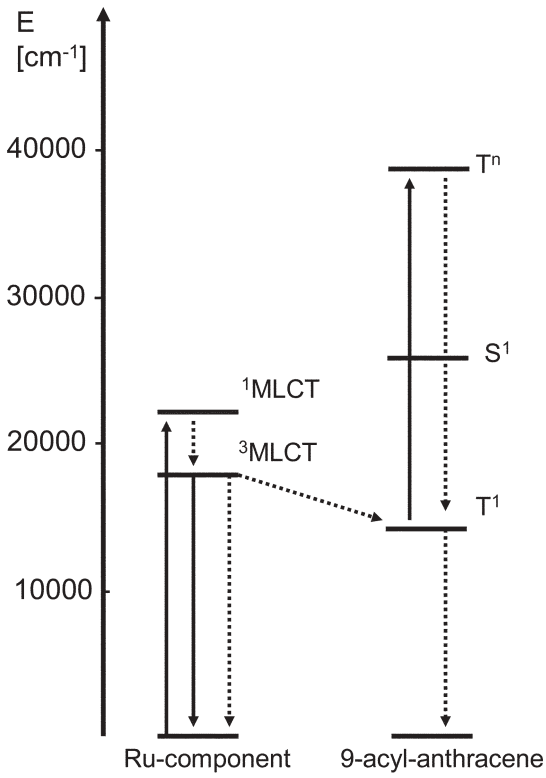

Fig. 29 Energy diagram of Ru-based component and 9-acyl-anthracene Full arrows indicate radiative processes, whereas dashed arrows represent radiationless pathways. Reprinted with permission from ref. 54. Copyright [2002] American Chemical Society Data.

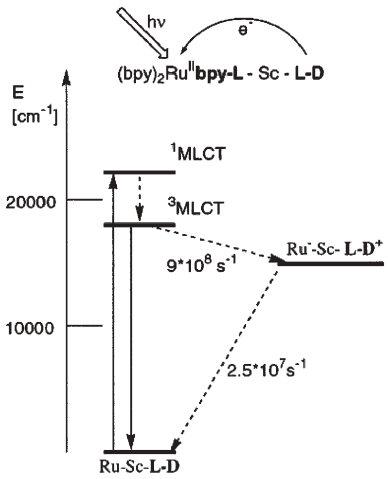

Fig. 30 Energy diagram of the assembly Ru-Sc-L-D with a schematic representation of the photoinduced electron-transfer process. Full arrows indicate radiative processes, whereas dashed arrows represent radiationless pathways. Reprinted with permission from ref. 54. Copyright [2002] American Chemical Society Data.

Energy transfer *via* cyclodextrin based supramolecular systems. The use of cyclodextrin as a template for the building of donor–acceptor supramolecular structures has been explored by De Cola, Pikramenou and co-workers, with respect to both vectorial energy[55] and electron transfer.[56] In contrast to systems based on hydrogen bonding, with cyclodextrins lipophylic interactions are employed to create supramolecular structure. This overcomes the inherent sensitivity to protic solvents observed with H-bonding systems (see previous section). These studies highlight the importance of understanding the nature of the donor and acceptor states in controlling both the direction and operating distance of energy and electron transfer.

The directionality of energy transfer is achieved through the use of different metal centres, Ru(II), Os(II) and Ir(II). The relative energies of the THEXI (thermally equilibrated excited) states (*e.g.* ^{3}MLCT, ^{3}IL) of the complexes are in the order Ir(III) > Ru(II) > Os(II). Hence by a suitable choice of the metal centre the direction of energy transfer in these systems can be controlled. However, the control over the effective distance of energy transfer is less straightforward. To a first approximation the energy transfer distance may be taken as the separation between the metal centres (*e.g.* the Ru(II) to Os(II) separation). However, this assumes that the donor and acceptor excited states are localised on the metal centres and while this may be a valid approximation for systems whose THEXI states are metal-based, it cannot hold where ligand based excited states (*e.g.* ^{3}MLCT and ^{3}IL) states are involved.

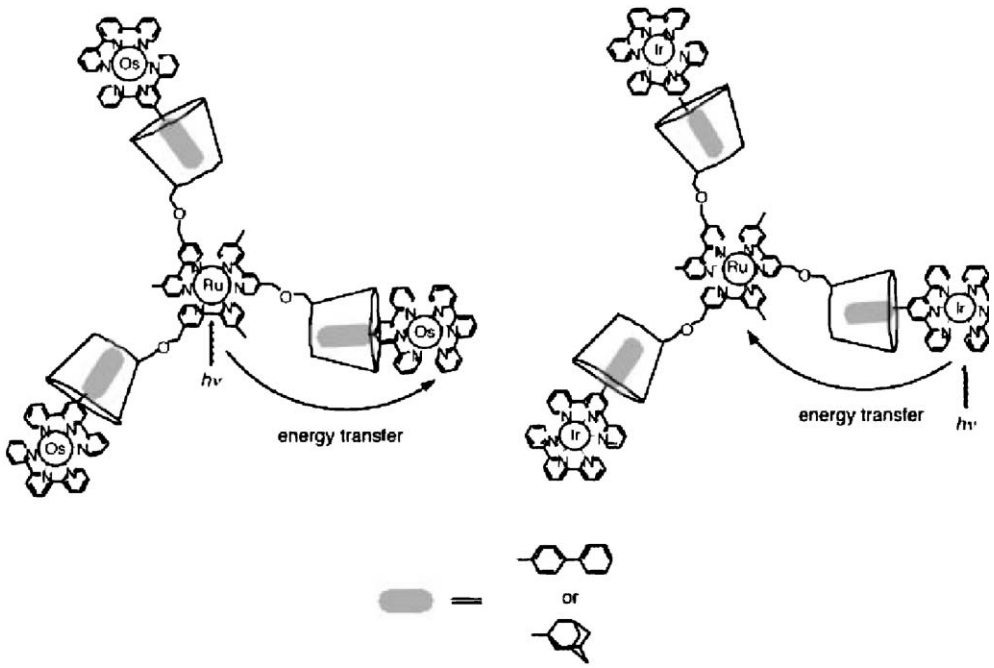

Fig. 31 Assemblied Os(II) or Ir(III) metal-complex guests with ruthenium based cyclodextrin host allows photoinduced energy transfer from and to the ruthenium core. Reprinted with permission from ref. 55*b*. Copyright [2003] John Wiley & Sons, Inc.

This latter point was exemplified in the use of adamantane and biphenyl units as 'anchors' for the cyclodextrin host cavities (Fig. 31). The use of biphenyl and adamantane represent two limiting situations. The aromatic biphenyl unit can engage in localisation of the ^{3}MLCT state of the guest molecule on the ligand closest to the cyclodextrin unit. However, in the case of adamantane components, the effect is to destabilise the ^{3}MLCT state of the ligand closest to the cyclodextrin, with the result that an excited state of the guest is localised on the peripheral unit. The consequences of these effects in terms of the effective energy transfer distance are potentially useful in modulating the energy transfer rates (through changes in donor–acceptor distance).

Photoinduced intermolecular electron transfer and EPR spectroscopy. Although, photoinduced intermolecular electron transfer is fundamental to the photosynthetic process and involves the generation of paramagnetic species, the use of EPR in photophysical studies of such systems has been very limited. The usefulness of EPR has been demonstrated by Styring and coworkers[57] and Shanzer *et al.*[19*b*] in studies of electron transfer between $[Ru(bipy)_3]^{2+}$ and dinuclear manganese complexes and dioxygen respectively. As discussed above (see section 2.1), following photo-excitation of $[Ru(bipy)_3]^{2+}$ (to $[Ru(bipy)_3]^{2+}$*), it becomes simultaneously a very strong reducing agent and a strong oxidant.[34]

Hence, in the excited state, outer sphere electron transfer processes, which are thermodynamically disfavoured ($\Delta G > 0$) in the ground state become energetically favoured in the excited state ($\Delta G < 0$). The paramagnetic species generated (*e.g.* Ru(III), Mn(III)Mn(IV)) are potentially sensitive to EPR spectroscopy allowing these photoinduced electron transfer processes to be monitored.

Conclusions and outlook

The above discussion provides a general, albeit brief, overview of the very extensive research that is going on into the structural and dynamic aspects of intercomponent interactions in multi-component systems. The central point is that, in order to elucidate the often complex nature of intercomponent processes, which occur in both multi-component molecular and supramolecular assemblies, it is important that as many different techniques as possible be brought to bear on the issues involved. When examining energy and electron transfer interactions, principal among the parameters to be considered are the energies of donor/acceptor excited state levels, the redox properties and also the distance between the interacting orbitals. In mixed ligand complexes it is first of all important to determine the nature of the excited state so that the efficiency of the exchange process and the distance between two interacting components can be established. However, the importance of donor–acceptor separation distance is not always appreciated fully. In Fig. 32 a number of theoretically possible interactions are shown. It is clear that the distance between the interacting components will be a key factor in determining the extent of interaction between them. For example, energy transfer between two polypyridyl moieties connected by a bridging ligand will be determined by the nature of the lowest energy excited state and whether it is based on the peripheral ligands or on the bridging ligand. It is also important to point out that the interaction mechanism in the ground state may be different from that obtaining in the excited state. For instance, the interaction between metal centres in intervalence compounds in the ground state may involve very different orbitals from those implicated in the excited state, particularly when this ground state interaction

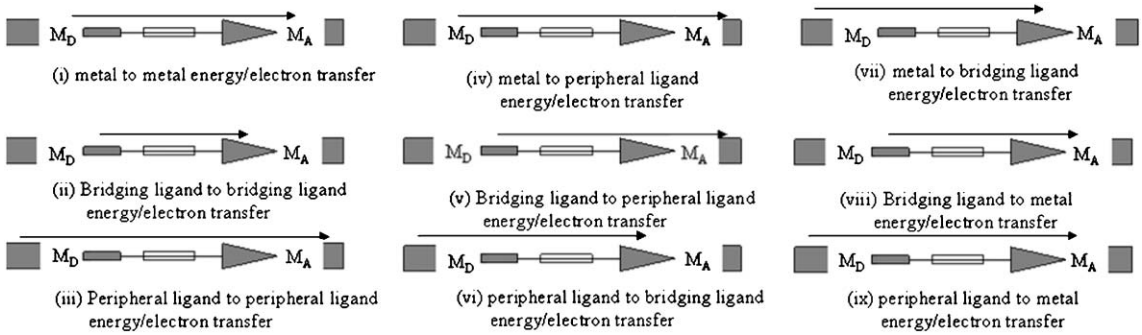

Fig. 32 Dependence of energy transfer distance on location of donor and acceptor moieties in a multi-component system

takes place *via* a HOMO based hole transfer mechanism and the excited state interaction is *via* LUMO orbitals located on peripheral ligands.

Several of the examples discussed in section 4 above also serve to emphasise the fact that the information derived from relevant experiments can enable the interaction between components in supramolecular assemblies to be tuned. Although molecular-based multicomponent systems have been at the forefront of investigations into energy and electron transfer processes, the growth of interest in nano-materials and in particular in heterogenous photonic devices will almost certainly lead to increased interest in molecular interactions with solid substrates such as TiO_2. When substrates such as the latter are actively involved, *i.e.* when particular surface states are available for population, hybrid, solid-molecular components or heterosupramolecular systems are created, which can be expected to behave very differently from solution-based analogues. Nevertheless the broad experimental and computational approaches taken in such studies are unlikely to be substantially different to those taken in the investigation of molecular systems.

References

1 (*a*) V. Balzani and F. Scandola, *Supramolecular Chemistry*, Ellis Horwood, New York, (1991); (*b*) B. Schlicke, L. De Cola, P. Belser and V. Balzani, *Coord. Chem. Rev.*, 2000, **208**, 267.
2 V. Balzani, P. Ceroni, A. Juris, M. Venturi, S. Campagna, F. Puntoriero and S. Serroni, *Coord. Chem. Rev.*, 2001, **219**, 545.
3 V. Balzani, A. Juris, M. Venturi, S. Campgna and S. Serroni, *Chem. Rev.*, 1996, **96**, 759.
4 Excited state proton transfer is beyond the scope of this review. See for example: L. M. Tolbert and K. M. Solntsev, *Acc. Chem. Res.*, 2002, **35**, 19.
5 (*a*) T. J. Meyer, *Acc. Chem. Res.*, 1978, **11**, 94; (*b*) P. Chen and T. J. Meyer, *Chem. Rev.*, 1998, **98**, 1439.
6 (*a*) P. Piotrowiak, *Chem. Soc. Rev.*, 1999, 143; (*b*) J.-P. Launay, *Chem. Soc. Rev.*, 2001, 386; (*c*) M. D. Ward, *Chem. Soc. Rev.*, 1997, 365 and references therein.
7 (*a*) Th. Forster, *T. Ann. Phys. (Liepzig)*, 1948, **2**, 55; (*b*) D. L. Dexter, *J. Chem. Phys.*, 1953, **21**, 836–850; (*c*) M. R. Wasielewski, *Chem. Rev.*, 1992, **92**, 435–461 and references therein.
8 J. P. Paris and W. W. Brandt, *J. Am. Chem. Soc.*, 1959, **81**, 5001.
9 (*a*) H. Yersin, W. Humbs and J. Strasser, *Topics Curr. Chem.*, 1997, **191**, 154; (*b*) H. Riesen and E. Krauz, *Comments Coord. Chem.*, 1995, **18**, 27; (*c*) H. Riesen and E. Krauz, *Int. Rev. Phys. Chem.*, 1997, **16**, 291.
10 Considerable interest remains in the early picosecond processes that lead to the lowest emissive states. see for example: (*a*) F. Puntoriero, S. Serroni, M. Galletta, A. Juris, A. Licciardello, C. Chiorboli, S. Carnpagna and F. Scandola, *Chem. Phys. Phys. Chem.*, 2005, **6**, 129; (*b*) G. B. Shaw, D. J. Styers-Barnett, E. Z. Gannon, J. C. Granger and J. M. Papanikolas, *J. Phys. Chem. A*, 2004, **108**, 4988; (*c*) S. A. McFarland, F. S. Lee, K. A. W. Y. Cheng, F. L. Cozens and N. P. Schepp, *J. Am. Chem. Soc.*, 2005, **127**, 7065.
11 M. Kasha, *Discuss. Faraday Soc.*, 1950, **9**, 14.
12 Energy transfer process through higher energy states, such as the 1MLCT states populated initially have recently been implicated in ultrafast energy and electron processes. See for example ref. 10a.
13 Usually referred to as, metal to metal charge transfer (MMCT), intervalence transition (IT), intervalence charge transfer (IVCT); in this review the abbreviation (IT) is used for convenience.
14 (*a*) G. D. Scholes, *Ann. Rev. Phys. Chem.*, 2003, **54**, 57; (*b*) K. F. Wong, B. Bagchi and P. J. Rossky, *J. Phys. Chem. A.*, 2003, **108**, 5752.
15 (*a*) N. S. Hush, *Prog. Inorg. Chem.*, 1967, **8**, 391; (*b*) N. S. Hush, *Chem. Phys.*, 1975, **10**, 361; (*c*) M. P. Robin and P. Day, *Adv. Inorg. Chem. Radiochem.*, 1967, **10**, 247–422.
16 (*a*) W. R. Browne, F. Weldon, A. Guckian and J. G. Vos, *Collect. Czech. Chem. Commun.*, 2003, **68**, 1467; (*b*) C. Di Pietro, S. Serroni, S. Campagna, M. T. Gandolfi, R. Ballardini, S. Fanni, W. R. Browne and J. G. Vos, *Inorg. Chem.*, 2002, **41**, 2871; (*c*) F. Weldon, L. Hammarström, E. Mukhtar, R. Hage, E. Gunneweg, J. G. Haasnoot, J. Reedijk, W. R. Browne, A. L. Guckian and J. G. Vos, *Inorg. Chem.*, 2004, **43**, 4471.
17 K. D. Demadis, C. M. Hartshorn and T. J. Meyer, *Chem. Rev.*, 2001, **101**, 2655–2686.
18 W. R. Browne and J. G. Vos, *Coord. Chem. Rev.*, 2001, **219**, 761.
19 (*a*) M. Asano-Someda, T. Ichino and Y. Kaizu, *J. Phys. Chem. A.*, 1997, **101**, 4484; (*b*) E. Yavin, L. Weiner, R. Arad-yellin and A. Shanzer, *J. Phys. Chem. A.*, 2001, **105**, 8018.
20 (*a*) T. Förster, *Z. Electrochem.*, 1950, **54**, 531; (*b*) J. F. Ireland and P. A. H. Wyatt, *Adv. Phys. Org. Chem.*, 1976, **12**, 131; (*c*) J. G. Vos, *Polyhedran*, 1992, **11**, 2285.
21 S. Goswami, R. Mukherjee and A. Chakravorty, *Inorg. Chem.*, 1983, **22**, 20, 2825.
22 M. D. Ward and J. A. McCleverty, *Dalton Trans.*, 2002, 275.
23 (*a*) D. F. Morris and W. H. Woodruff, in *Spectroscopy of Inorganic Based materials*, R. J. H. Clark and R. E. Hester, Eds.; John Wiley & Sons: New York, 1987; (*b*) D. P. Strommen and K. Nakamoto, *J. Chem. Educ.*, 1977, **54**, 474; (*c*) S. E. J. Bell, *The Analyst*, 1996, **121**, 107R; (*d*) J. J. McGarvey, P. Callaghan, C. G. Coates, J. R. Schoonover, J. M. Kelly, L. Jacquet and K. C. Gordon, *J. Phys. Chem. B.*, 1998, **102**, 5941; (*e*) J. R. Ferraro and K. Nakamoto, *Introductory Raman Spectroscopy*, Academic Press Limited, London, (1994).
24 T. Kuwana and W. R. Heineman, *Acc. Chem. Res.*, 1976, **9**, 241.
25 R. Hage, J. G. Haasnoot, H. A. Niewenhuis, J. Reedijk, D. H. De Ridder, J. G. Vos and R. Wang, *J. Am. Chem. Soc.*, 1990, **112**, 9245.
26 (*a*) J. Terner and M. A. El-Sayed, *Acc. Chem. Res.*, 1985, **18**, 331; (*b*) J. R. Schoonover and G. F. Strouse, *Chem. Rev.*, 1998, **98**, 1335; (*c*) M. K. Kuimova, W. Z. Alsindi, J. Dyer, D. C. Grills, O. S. Jina, P. Matousek, A. W. Parker, P. Portius, X. Z. Sun, M. Towrie, C. Wilson, J. X. Yang and M. W. George, *Dalton Trans.*, 2003, **21**, 3996.
27 C. E. Banks, N. V. Rees and R. G. Compton, *J. Phys. Chem. B.*, 2002, **106**, 5810.

28 (*a*) C. J. Kleverlaan, D. J. Stufkens, I. P. Clark, M. W. George, J. J. Turner, D. M. Martino, H. van Willigen and A. Vlcek, Jr., *J. Am. Chem. Soc.*, 1998, **120**, 10871; (*b*) J. Dyer, W. J. Blau, C. G. Coates, C. M. Creely, J. D. Gavey, M. W. George, D. C. Grills, S. Hudson, J. M. Kelly, P. Matousek, J. J. McGarvey, J. McMaster, A. W. Parker, M. Towrie and J. A. Weinstein, *Photochem. Photobiol. Sci.*, 2003, **2**, 542; (*c*) H. A. Niewenhuis, D. J. Stufkens, R. A. McNicholl, A. H. R. Al-Obaidi, C. G. Coates, S. E. J. Bell, J. J. McGarvey, J. Westwell, M. W. George and J. J. Turner, *J. Am. Chem. Soc.*, 1995, **117**, 5579.

29 There is a certain amount of debate in the literature as to whether or not DFT methods are truly *ab-initio*. In reality, it depends on the functional chosen, as some (*e.g.* the hybrid B3LYP) are parameterised using empirical data (from the He atom in the case of the LYP functional), although only a fraction of the parameters used in semi-empirical calculations are employed. Other functionals do not require any experimentally derived data for parameterisation and are therefore *ab-initio* methods. In this review, DFT is described as being *ab-initio* as this is the convention – although strictly speaking not true in all cases.

30 (*a*) F. M. Bickelhaupt and E. J. Baerends, *Rev. Comput. Chem.*, 2000, **15**, 1; (*b*) W. Kohn and L. J. Sham, *Phys. Rev. A*, 1965, **140**, 1133.

31 (*a*) P. Hohenberg and W. Kohn, *Phys. Rev.*, 1964, **136**, B864; (*b*) O. Gunnarson and B. I. Lundqvist, *Phys. Rev. B*, 1976, **13**, 4274; (*c*) O. Gunnarson and B. I. Lundqvist, *Phys. Rev. B*, 1976, **15**, 6006 (erratum).

32 (*a*) J.-F. Guillemoles, V. Barone, L. Joubert and C. Adamo, *J. Phys. Chem. A*, 2002, **106**, 11354; (*b*) I. Ciofini, C. A. Daul and C. Adamo, *J. Phys. Chem. A*, 2003, **107**, 11182; (*c*) G. Pourtois, D. Beljonne, C. Moucheron, S. Schumm, A. Kirsch-De Mesmaeker, R. Lazzaroni and J.-L. Brédas, *J. Am. Chem. Soc.*, 2004, **126**, 683–692.

33 (*a*) T. Ziegler, A. Rauk and E. J. Baerends, *Theor. Chim. Acta*, 1977, **43**, 26; (*b*) C. Daul, *Int. J. Quantum Chem.*, 1994, **52**, 867.

34 A. Juris, V. Balzani, F. Barigelletti, S. Campagna, P. Belser and A. von Zelewsky, *Coord. Chem. Rev.*, 1988, **84**, 85–277.

35 J. G. Vos, *Polyhedron*, 1992, **11**, 2285.

36 (*a*) G. D. Danzer and J. R. Kincaid, *J. Phys. Chem.*, 1990, **94**, 3976–3980; (*b*) G. D. Danzer, J. A. Golus and J. R. Kincaid, *J. Am. Chem. Soc.*, 1993, **115**, 8643.

37 T. E. Keyes, C. M. O'Connor, U. O'Dwyer, C. G. Coates, P. Callaghan, J. J. McGarvey and J. G. Vos, *J. Phys. Chem. A.*, 1999, **103**, 8915.

38 The emission lifetime of the Hpytr complex is to short to be measured (<10 ns).

39 J. V. Caspar and T. J. Meyer, *J. Phys. Chem.*, 1983, **87**, 952.

40 C. Daul, E. J. Baerends and P. Vernooijs, *Inorg. Chem.*, 1994, **33**, 3538.

41 (*a*) J. E. Monat, J. H. Rodriguez and J. K. McCusker, *J. Phys. Chem. A*, 2002, **106**, 7399; (*b*) F. Aiga and T. Tada, *J. Mol. Struct.*, 2003, **658**, 25; (*c*) H. Zabri, I. Gillaizeau, C. A. Bignozzi, S. Caramori, M.-F. Charlot, J. Cano-Boquera and F. Odobel, *Inorg. Chem.*, 2003, **42**, 6655; (*d*) F. De Angelis, S. Fantacci and A. Selloni, *Chem. Phys. Lett.*, 2004, **389**, 204; (*e*) S. I. Gorelsky, A. B. P. Lever and M. Ebadi, *Coord. Chem. Rev.*, 2002, **230**, 97.

42 A. Amini, A. Harriman and A. Mayeux, *Phys. Chem. Chem. Phys.*, 2004, **6**, 1157.

43 (*a*) A. Broo and P. Lincoln, *Inorg. Chem.*, 1997, **36**, 2544; (*b*) H. Masui, A. L. Freda, M. C. Zerner and A. B. P. Lever, *Inorg. Chem.*, 2000, **39**, 141; (*c*) A. DelMedico, E. S. Dodsworth, A. B. P. Lever and W. J. Pietro, *Inorg. Chem.*, 2004, **43**, 2654–2671; (*d*) H. Rensmo, S. Lunell and H. Siegbahn, *J. Photochem. Photobiol. A*, 1998, **114**, 117; (*e*) R. A. Metcalfe, L. C. G. Vasconcellos, H. Mirza, D. W. Franco and A. B. P. Lever, *J. Chem. Soc., Dalton Trans.*, 1999, 2653.

44 M. Buchs and C. Daul, *Chimia*, 1998, **52**, 163.

45 W. R. Browne, N. M. O'Boyle, W. Henry, A. L. Guckian, S. Horn, T. Fett, C. M. O'Connor, M. Duati, L. De Cola, C. G. Coates, K. L. Ronayne, J. J. McGarvey and J. G. Vos, *J. Am. Chem. Soc.*, 2005, **127**, 1229.

46 R. H. Laye, S. M. Couchman and M. D. Ward, *Inorg. Chem.*, 2001, **40**, 4089.

47 C. G. Coates, T. E. Keyes, H. P. Hughes, P. M. Jayaweera, J. J. McGarvey and J. G. Vos, *J. Phys. Chem. A.*, 1998, **102**, 5013.

48 M. D. Ward and F. Barigelletti, *Coord. Chem. Rev.*, 2001, **216**, 127.

49 M. T. Indelli, C. A. Bignozzi, A. Harriman, J. R. Schoonover and F. Scandola, *J. Am. Chem. Soc*, 1994, **116**, 3768.

50 E. C. Constable, R. W. Handel, C. E. Housecroft, A. F. Morales, L. Flamigni and F. Barigelletti, *Dalton Trans.*, 2003, 1220.

51 N. M. Shavaleev, Z. R. Bell, T. L. Easun, R. Rutkaite, L. Swanson and M. D. Ward, *Dalton Trans.*, 2004, **21**, 3678.

52 S. Rau, B. Schäfer, S. Schebesta, A. Grüßing, W. Poppitz, D. Walther, M. Duati, W. R. Browne and J. G. Vos, *Eur. J. Inorg. Chem.*, 2003, 1503.

53 P. D. Beer, F. Szemes, P. Passaniti and M. Maestri, *Inorg. Chem.*, 2004, **43**, 3965.

54 M. Kercher, B. König, H. Zieg and L. De Cola, *J. Am. Chem. Soc.*, 2002, **124**, 11541.

55 (*a*) J. M. Haider, M. Chavarot, S. Weidner, I. Sadler, R. M. Williams, L. De Cola and Z. Pikramenou, *Inorg. Chem.*, 2001, **40**, 3912; (*b*) J. M. Haider, R. M. Williams, L. De Cola and Z. Pikramenou, *Angew. Chem. Int. Ed.*, 2003, **42**, 1830.

56 H. F. M. Nelissen, M. Kercher, L. De Cola, M. C. Feiters and R. J. M. Nolte, *Chem. Eur. J.*, 2002, **8**, 5407.

57 (*a*) P. Huang, A. Magnuson, R. Lomoth, M. Abrahamson, M. Tamm, L. Sun, B. van Rotterdam, J. Park, L. Hammarstrom, B. Akermark and S. Styring, *J. Inorg. Biochem.*, 2002, **91**, 159; (*b*) P. Huang, J. Hogblom, M. F. Anderlund, L. Sun, A. Magnuson and S. Styring, *J. Inorg. Biochem*, 2004, **98**, 733.

58 M. J. Frisch, G. W. Trucks, H. B. Schlegel, G. E. Scuseria, M. A. Robb, J. R. Cheeseman, J. A. Montgomery, Jr., T. Vreven, K. N. Kudin, J. C. Burant, J. M. Millam, S. S. Iyengar, J. Tomasi, V. Barone, B. Mennucci, M. Cossi, G. Scalmani, N. Rega, G. A. Petersson, H. Nakatsuji, M. Hada, M. Ehara, K. Toyota, R. Fukuda, J. Hasegawa, M. Ishida, T. Nakajima, Y. Honda, O. Kitao, H. Nakai, M. Klene, X. Li, J. E. Knox, H. P. Hratchian, J. B. Cross, V. Bakken, C. Adamo, J. Jaramillo, R. Gomperts, R. E. Stratmann, O. Yazyev, A. J. Austin, R. Cammi, C. Pomelli, J. Ochterski, P. Y. Ayala, K. Morokuma, G. A. Voth, P. Salvador, J. J. Dannenberg, V. G. Zakrzewski, S. Dapprich, A. D. Daniels, M. C. Strain, O. Farkas, D. K. Malick, A. D. Rabuck, K. Raghavachari, J. B. Foresman, J. V. Ortiz, Q. Cui, A. G. Baboul, S. Clifford, J. Cioslowski, B. B. Stefanov, G. Liu, A. Liashenko, P. Piskorz, I. Komaromi, R. L. Martin, D. J. Fox, T. Keith, M. A. Al-Laham, C. Y. Peng, A. Nanayakkara, M. Challacombe, P. M. W. Gill, B. G. Johnson, W. Chen, M. W. Wong, C. Gonzalez and J. A. Pople, *GAUSSIAN 03 (Revision B.04)*, Gaussian, Inc., Pittsburgh, PA, 2003.

59 We have developed a tool, GaussSum, that automates the creation of EDDMs using the output of a Gaussian03 TDDFT calculation. N. M. O'Boyle and J. G. Vos, *GaussSum 0.8*; Dublin City University, 2004.

60 W. Humphrey, A. Dalke and K. Schulten, *J. Mol. Graph.*, 1996, **14**, 1, 33.

61 S. Anger, S. A. Bennett, D. K. Buck, A. A. Collins, A. Enzmann, D. Farmer, D. Muir, B. Pulver, R. Skinner, S. Taylor, D. Wells and C. Young, *Persistance of Vision Raytracer, Official version 2.2*, 1993, http://www.povray.org.